A Review of *In Vitro* Instrumentation Platforms for Evaluating Thermal Therapies in Experimental Cell Culture Models

Faraz Chamani,[a] India Barnett,[a] Marla Pyle,[b] Tej Shrestha,[b,c] & Punit Prakash[a,*]

[a]Department of Electrical and Computer Engineering, Kansas State University, Manhattan, KS, USA; [b]Department of Anatomy and Physiology, College of Veterinary Medicine, Kansas State University, Manhattan, KS, USA; [c]Nanotechnology Innovation Center of Kansas State (NICKS), Kansas State University, Manhattan, KS, USA

*Address all correspondence to: Punit Prakash, Department of Electrical and Computer Engineering, Kansas State University, 3078 Engineering Hall, Manhattan, KS 66506; Tel.: +785-532-5600; Fax: +785-532-1188, E-mail: prakashp@ksu.edu

ABSTRACT: Thermal therapies, the modulation of tissue temperature for therapeutic benefit, are in clinical use as adjuvant or stand-alone therapeutic modalities for a range of indications, and are under investigation for others. During delivery of thermal therapy in the clinic and in experimental settings, monitoring and control of spatio-temporal thermal profiles contributes to an increased likelihood of inducing desired bioeffects. *In vitro* thermal dosimetry studies have provided a strong basis for characterizing biological responses of cells to heat. To perform an accurate *in vitro* thermal analysis, a sample needs to be subjected to uniform heating, ideally raised from, and returned to, baseline immediately, for a known heating duration under ideal isothermal condition. This review presents an applications-based overview of *in vitro* heating instrumentation platforms. A variety of different approaches are surveyed, including external heating sources (i.e., CO_2 incubators, circulating water baths, microheaters and microfluidic devices), microwave dielectric heating, lasers or the use of sound waves. We discuss critical heating parameters including temperature ramp rate (heat-up phase period), heating accuracy, complexity, peak temperature, and technical limitations of each heating modality.

KEY WORDS: hyperthermia, *in vitro* heating, cancer cells, cell death, protein expression kinetics, predictive models

I. INTRODUCTION

Hyperthermia refers to heating the target cells or biological tissues to temperatures exceeding physiologic temperature. Heating induces a number of local and systemic effects, from the macroscopic tissue level down to the sub-cellular molecular level, which may be harnessed for cancer therapy. The specific changes induced by heating are a function of the spatio-temporal temperature profiles induced in tissue during treatment. In addition to cytotoxicity,[1] mild hyperthermia, 39–42°C delivered for > 30 min, induces tumor reoxygenation,[2,3] improves drug delivery,[4,5] activates promoters for gene therapy,[6,7] augments anti-tumor immunity,[8–10] and sensitizes cancer cells to DNA damaging agents by inhibiting DNA repair, supporting the hypothesis that repair pathways can be affected by heat.[11,12] Multiple phase II/III clinical trials have demonstrated the benefit of combining hyperthermia with chemo/radiation therapies in patients with different types of cancer, showing a significant enhancement in treatment effectivity without significant toxicity effects.[11,13–15] Compared with mild hyperthermia as an adjuvant therapeutic option, high temperature thermal ablation (T > 50°C) is increasingly being used for *in situ* destruction of unresectable localized tumors.[16] Elevated temperatures can affect cells in different ways, but the primary means of cell death during thermal ablation is acute coagulative necrosis. Beyond the boundary of the ablation zone, tissue temperatures fall within the mild hyperthermia range and thus provide a potential opportunity for cells to be more susceptible to other therapeutic modalities.[17,18] Conversely, some studies have described the potential of extended mild hyperthermic (i.e. sub-ablative) heating at the tumor-normal tissue boundary contributing to the promotion of distant tumor growth.[19] Thus, the effects of mild hyperthermia on normal and malignant cells are also of high relevance to thermal ablation.

0278-940X/22/$35.00

With the development and ongoing clinical translation of several thermal therapy delivery modalities [e.g., magnetic resonance guided high-intensity focused ultrasound (FUS), nanoparticle mediated laser therapy, probe-based radiofrequency and microwave (MW) hyperthermia/ablation], combining heat with other cancer therapeutic strategies, including immunotherapy and gene therapy, has remained an area of research investigation. For instance, thermally-sensitive microbubbles and nanoparticles are being explored for highly selective delivery of drugs and other therapeutic agents to targeted tissue.[5,20] The augmented immune response elicited by thermal ablation is being investigated to boost the efficacy of immunotherapy strategies, thereby enabling local control of tumors and inducing sustained anti-tumor immunity.[21,22] However, there are few standardized quantitative assessment tools linking heating profiles to local and systemic effects of heat in combination with other therapeutic modalities. The availability of such tools would pave the way for the design of customized patient-specific heating strategies that optimize specific physiological responses to heat for synergy with other treatments.

The local effects induced by a thermal therapy procedure are strongly dependent on the spatio-temporal temperature profiles achieved during treatment.[23,24] Mathematical models provide a powerful tool for quantitatively assessing the physiological responses to heat treatment across multiple spatial and temporal scales. These models rely on underlying experimental data characterizing bioeffects (e.g., cell viability, stress protein expression) as a function of intensity and duration of heating. *In vitro* platforms of cells in culture (2D and 3D) provide a powerful experimental approach for investigating bioeffects of heating across a variety of cell lines. These experimental platforms rely on isothermal heating of cells for known duration of times to facilitate development of quantitative models of the bioeffects of heating. In quantitative analysis of cellular reactions, it is usually analyzed what happens under isothermal conditions and then consider the bioeffects of temperature. In isothermal methods, it is assumed that bioeffects that are induced by the transient portion of the thermal history are negligible compared to those induced by the isothermal portion. Therefore, caution should be taken to account for potential thermal injury during the ramping and cooling phases.

In vitro studies are highly informative for gaining an understanding of the myriad biological effects of hyperthermia exposures at the cellular level, such as cytotoxicity effects at different temperatures and exposure times, as well as their influence on the efficacy of other therapeutic modalities. An advantage of the *in vitro* setting is the more controlled environment they provide, compared with *in vivo* setting where there are considerably more sources of heterogeneity within and across subjects. This controlled environment can be particularly helpful for detailed investigation of multi-modality therapeutic strategies. Moreover, *in vitro* evaluation of hyperthermia exposure parameters may help guide the development of predictive models and protocols for investigation in future *in vivo* studies. For example, Tang et al. conducted an *in vitro* study investigating the synergistic effect between hyperthermia and chemotherapy on ovarian cancer cells. In their study, hyperthermia in combination with chemotherapeutic drugs resulted in significant increase in cell death when compared with chemotherapy alone, providing a valuable tool for cancer treatment.[25]

For the quantitative analysis of bioeffects of heating, it is informative to distinguish between effects as a function of intensity of heating (i.e., temperature) alone vs. the intensity and duration of heating (i.e., time - temperature history).[26] For this reason, *in vitro* systems aim to provide rapid heating to target temperatures that approach the ideal, but not practically feasible isothermal heating. By assessing bioeffects at a number of combinations of target temperatures and heating time, the kinetic parameters of bioeffects can be determined for estimating the impact of non-isothermal thermal profiles. It is noted that during *in vivo* exposures, iso-thermal exposures are seldom achievable; different rates of heating are likely to be observed in varying regions of the targeted tissue. Tang et al. compared the synergistic effects of two different heating methods, laser induced rapid rate heating and incubator induced slow rate heating. The IC_{50} value of the combined chemotherapeutic drug was lower with only 1

minute of laser induced fast heating when compared with 60 minutes of incubator induced slow heating on ovarian cancer cells, highlighting the importance of heating rate when cancer cells are subjected to hyperthermia treatments.[27]

In vitro heating can be delivered using different strategies; the vast majority of studies employed conductive and convective processes using circulating water baths and CO_2 incubators.[28–32] Recently, other modalities have been developed to deliver *in vitro* heating, including: Joule heating,[33,34] microwaves,[35–38] lasers,[39–42] alternating magnetic fields,[43,44] and ultrasound mediated heating.[45–47] Achieved peak temperature, accuracy of heating, and technical limitations may vary significantly depending on the selected heating approach. Traditional heating modalities such as water baths and incubators facilitate uniform temperature regulation with a high degree of accuracy and simplicity; however heating rate is slow, limiting the opportunity to study the mechanisms of heat-induced cellular response. Accurate control of cell culture temperature provides several opportunities to study the temperature-dependent cellular responses. For example, it enables one to characterize transient response of cells during heating and cooling phases, or to determine a thermal dose threshold necessary for the heat-induced cell death.[48–50] Characteristics of *in vitro* hyperthermia exposure apparatus include: (1) high temperature ramp rate (the time to reach the target temperature) and/or short heat-up phase; (2) precise control of temperature with high degree of accuracy; (3) homogeneous heating pattern throughout the sample area, and (4) simple design and being easy to use.

The objective of the present review is to provide an overview of currently available *in vitro* heating modalities and recent advances in the field. All reported techniques along with the corresponding specifications (heat-up phase, heating accuracy, complexity, peak temperature and heating limitations), are summarized in Table 1 where "T_{Output}" denotes obtained sample temperature, "$T_{Initial}$" is the initial temperature of the sample prior to heating, "Input" is the input signal (e.g. power, temperature, voltage), "Accuracy" is the accuracy of temperature control during heating, "Uniformity" is temperature distribution homogeneity during heating, and "$N_{Sensors}$" describes number of temperature sensors that was used in each heating system. We also provided an assessment of the relative complexity of each system, based on the number of elements required to assemble the overall system, and our assessment of the challenges with doing so. For each of the above parameters, if the original reference did not provide information to assess that parameter, the term "NA" (not available) was used in Table 1.

II. OVERVIEW OF HEATING METHODS

A. CO_2 Incubators

Temperature-controlled CO_2 incubators, which are routinely used for providing a controlled environment for culturing cells, have been adapted as a primary heating source for *in vitro* hyperthermia studies.[29,51,52] Convective heat exchange between cells in culture and the air in the incubator provides a means for heating; however, the air temperature within the incubator may not be stable when the incubator door is opened to move the plates in or out of the incubator, taking extended periods of time to stabilize. Consequently, this may lead to poor control of temperature during transient hyperthermia exposures. The incubator's specifications with respect to uniformity and temperature control fluctuation are normally within 0.25°C and 0.1°C, respectively. To directly record the sample temperature, thermocouples are inserted inside the cell culture dish during hyperthermia treatments. Nytko et al.[51] described such a system using a 5% CO_2 incubator, and reported that it took approximately 40 min for cells to achieve the hyperthermic temperature (42°C). Figure 1 illustrates the temperature profiles inside the culture dish that was measured in different runs.

Shellman et al.[29] also used a conventional CO_2 incubator to perform *in vitro* heating. They developed a heating system using multiple thermocouples (T-type) and measured the temperatures in multiple wells (Fig. 2). Temperature of sample that was controlled in their study was reported with 0.2°C of accuracy. As shown in Fig. 2, using custom made copper blocks in contact with the 96-well plate inside the incubator provided a significantly fast ramping rate with a heat-up phase of ~ 20 min to

TABLE 1: Comparative analysis of *in vitro* heating techniques and corresponding technical specifications

Cell carrier	Sample size	Heating modality	T_{Output} (°C)	Input	Ramping (s)	Accuracy (°C)	Uniformity (°C)	Complexity	$T_{Initial}$ (°C)	$N_{sensors}$ (#)
Petri-dish-10 cm[51]	10 mL	Incubator (not preheated)	41.5	42°C	2400	0.1−0.5	0.25	+	37	1
96 WP[29]	100 µL	Incubator (preheated)	47.2	48°C	1320	0.2−0.8	2	+	37	5
96 WP[29]	100 µL	Incubator (preheated)	47.2	48°C	3000	0.2−0.8	2	+	37	5
96 WP sealed[32]	200 µL	Water bath (immersed)	46.6	46.8°C	152	0.2	NA	++	22	2
96 WP sealed[32]	200 µL	Water bath (floating)	52.8	55.8°C	251	3	NA	++	22	2
0.5 mL PCR tube[32]	200 µL	Water bath (floating)	46.3	46.9°C	52	0.6	NA	++	22	2
96 WP-wrapped[29]	100 µL	Water bath (immersed)	48.6	48.6°C	1200	0.2	0.2	++	26	5
T25 Flask[57]	70 mL	Water bath (hot media injection)	49.5, 49.8	50°C	12, 60	0.2−0.5	NA	+++	37	2
96 WP[58]	100−200 µL	Water bath (hot PBS injection)	45−60	45−60°C	Instant	1.4	NA	+++	37	1
6 WP[61]	3 mL	MW	50	10−20 W	420−180	2	4	+++	25	4
48 WP[63]	500 µL	MW	50−60	15 W	30−50	NA	NA	+++	37	1
Beaker[103]	30 mL	MW	40−60	1−25 W	17−36	1	NA	+++	25	Self
Petri-dish-35 mm[62]	2.5 mL	MW	39.5	6.8 W	30	0.1−2.5	NA	++++	27	1+Self
Petri-dish-30 mm[40]	1.2 mL	Laser	40−60	3−16 W	10	NA	2−15	+++++	37	21
Petri-dish-35 mm[104]	1 mL	Laser	30	0.2 W	240	NA	2−6	+++++	22	1
48 WP[105]	150 µL	Laser	60	3.8 W/ cm^2	300	2	NA	++++++	37	1

TABLE 1: (*continued*)

Centrifugal tube[39]	75 µL	Laser	37–70	2 W	30–200	2	NA	+++	24	1
Collagen gel[45]	129 ×86 mm^2	Ultrasound	45	1100 W/ cm^2	300	NA	5	+++++	23	1
Agarose phantom[47]	20 × 75 mm^2	Ultrasound	45	4.4 MPa	6	NA	3–5	+++++	37	1
wells[46]	0.3 × 0.3 × 0.3 mm^3	Ultrasound	37	10 V	900	0.02	0.3	+++++	23	2
96 WP[76]	420 µL	Ultrasound	45	213W/ cm^2	120	2.29	NA	+++++	34	1
Agarose phantom[106]	25 × 25 × 20 mm^3	Ultrasound	30	1.54 MHz	70	1.1	4	+++++	22	3
Culture dish-60 mm[107]	30 mL	Microheater	37	5 W	240	2–3	NA	+++	32	1
Culture chamber[77]	1 mL	Microheater	37	2 W	1200	0.2–1.5	0.4–2.9	+++	24	Self
Culture chamber[108]	50 µL	Microheater	65	0.22 W	1800	5	10	+++	24	2
Culture chamber[81]	7.6 mm × 13 mm	Microheater	37	2.5 V	No heating	0.26	3	+++	37	Self
Glass slide[109]	20 µL	Microheater	50	1 V	4	0.5	10	+++	24	1
Chamber[91]	2–3 mL	Millifluidic device	43	3000 AU	0.3	1	0.5	++++	37	1
Eppendorf tube[92]	0.5–5 mL	Microfluidic device	37	0.65 W	210	0.2	0.5	+++++	36.5	1

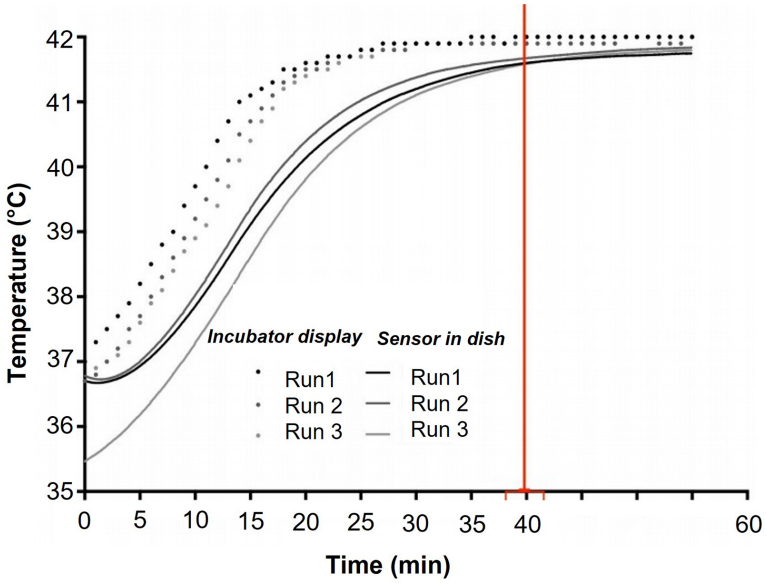

FIG. 1: Temperature profile of the incubator during heating from 37°C to 42°C steady state with three different runs. Dot makers show the temperature displayed by the incubator while the solid lines describe actual measured temperature of the sample based on three different runs inside cell culture dish (adapted from Nytko et al.).[51]

achieve desired hyperthermic temperature (in this case 48°C) while using no copper blocks during incubation led to a significantly longer heat-up phase (40 min). A technical obstacle in their study was that heating the cells with copper blocks in the incubator achieved 0.8°C less than of the desired hyperthermic temperature which can be resolved by adjusting the temperature setting in the incubator.

B. Water Baths

Many studies have used temperature-controlled water baths to heat cells *in vitro*.[19,28,53–56] Briefly, this method involves immersing the cells within the culture container into a water bath set at the desired hyperthermic temperature. An electronic interface in most water baths allows users to set a desired temperature. Figure 3 depicts the photograph of a temperature-controlled circulating water bath.

However, to prevent contamination of the cells in culture, the plates need to be sealed. The effects of lower CO_2 levels in the media accompanying long incubation time can affect cell viability in some cell types as previously described by Shellman et al.[29] Another challenge with the water bath heating technique is that the cell culture plates heated in a water bath tend to have condensation on their lid that may cause inconsistency in the volume of the media of each well after heating. This can decrease the reproducibility of certain biological assays. It is recommended for the cell culture plates to be placed on a stand in the preheated water bath to avoid direct contact with the metal bottom of the water bath upon the immersion. This is to avoid adhesion of deposited chemical substances to the culture plates at the bottom of the water bath. The time constant for temperature equilibration through a plastic container is relatively slow (~ minutes), thus some studies have aimed to decrease this time by adding heated media at the desired target temperature to the sample, and then placing the container within the water bath to maintain temperature.[57,58]

Massey et al.[32] presented a method for measuring target engagement in adherent cells. In their study, a preheated water bath was used as the heat source for cells at the target temperature of 55°C. Meanwhile, the temperature changes inside the cell culture plates were determined by using two different thermocouples. The ramping rate to desired hyperthermic temperature was determined in both

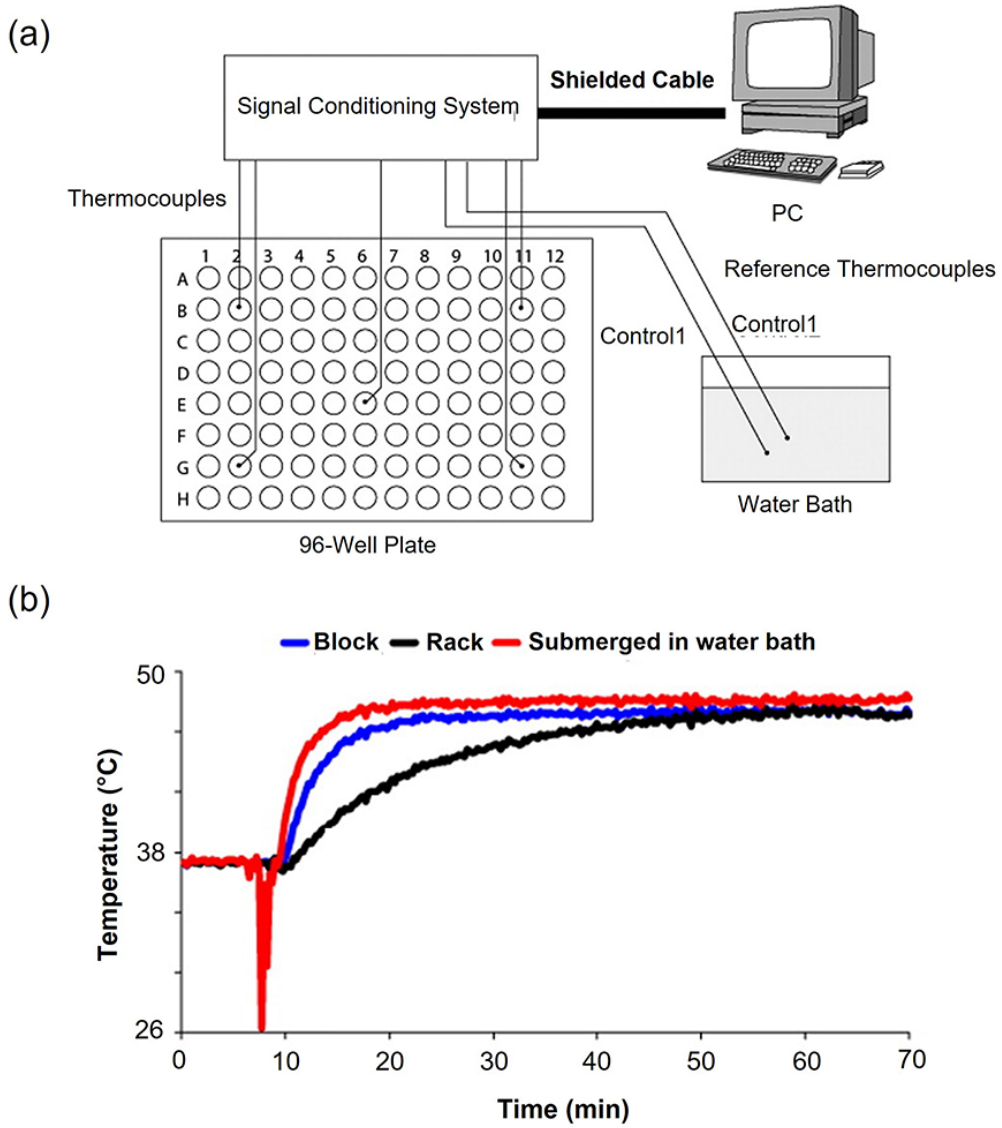

FIG. 2: (a) Equipment setup for temperature measurement of media in a 96-well plate consisting of five sealed thermocouples in different wells of the culture plate to monitor the actual sample temperature during hyperthermia exposure. (b) Average measured temperature based on five temperature probes sealed in different wells of a culture plate at each time point for different heating techniques (i.e. submerged in water bath, placed in incubator rack with no copper blocks and with copper blocks) (adapted from Shellman et al.[29]).

thin-walled PCR tube and 96-well plates, either floating or submerged in the preheated water bath (Fig. 4). The PBS in the PCR tube heated up rapidly reaching 54°C within 45 s. The heat-up phase to achieve a temperature of 54°C was 3 and 5.5-fold slower in a cell culture plate that was submerged and floating in a preheated water bath, respectively.

Similarly, Rylander et al.[57] used a constant temperature circulating water bath as a heat source to identify elevated levels of heat shock proteins following hyperthermia exposures. Two K-type thermocouples were used on 25 cm^2 phenolic flask containing cell culture medium and recorded the temperature during heat exposure in the bottom and

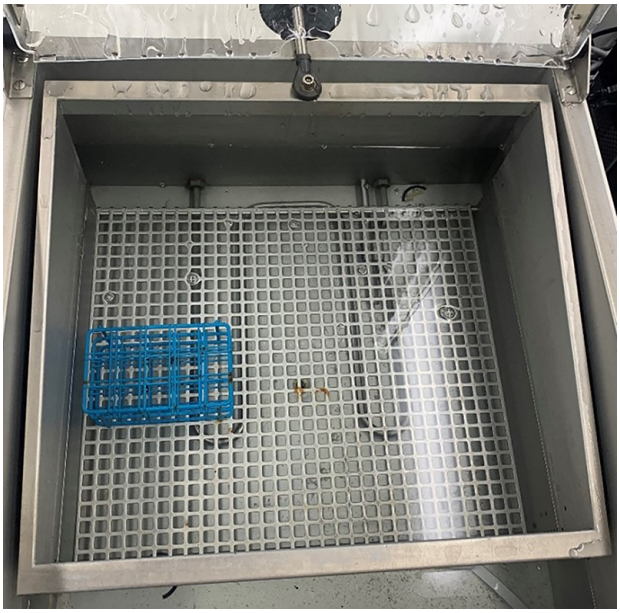

FIG. 3: Photographic appearance of a water bath system

inside the culture medium. The flask was then filled with 70 ml of heating medium (0.1°C equilibrium) and immersed in the water bath for different durations (1–30 min). Samples were subjected to temperatures of 44, 46, 48, and 50°C with six samples for each time increments. A relatively fast temperature ramping rate (~ 4 s) was obtained, achieving ~ 63% of the desired hyperthermic temperature. Temperature of cells was estimated as the average of bottom wall and culture medium values and reached within 0.5°C and 0.2°C of desired hyperthermic temperature in 12 s and 60 s, respectively.

C. Electromagnetic Radiation

Conventional incubators, such as dry air ovens, heating blocks and water baths, rely on conductive and convective processes for heat transfer. The techniques described in this section involve active

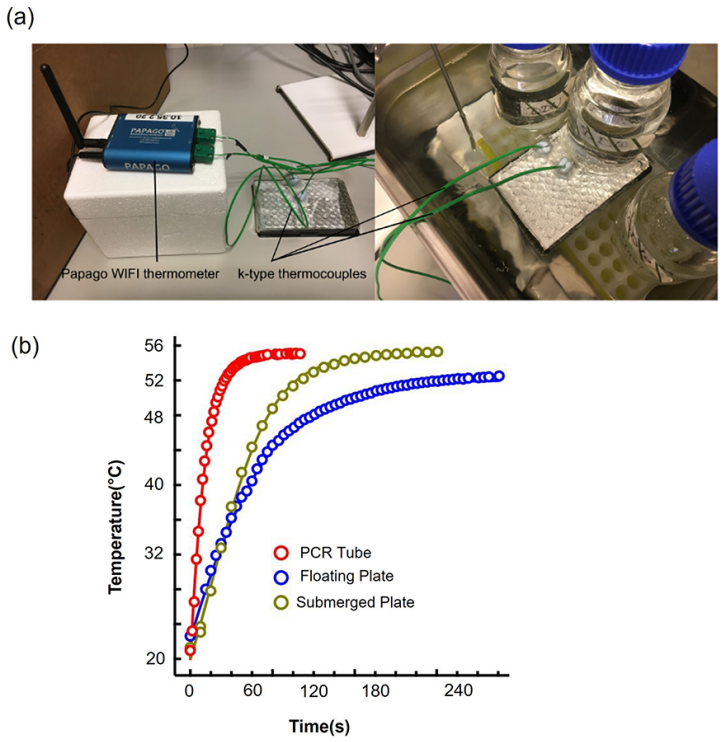

FIG. 4: (a) Thermometer set up with two k-type thermocouples placed in a cell carrier-96 plate that was sealed with an aluminum plate sealer and was heated by immersion in the water bath. (b) measured sample temperature following floating and submerged cell carrier-96 plate in a preheated water bath at 55°C, shown by blue color (Floating Plate) and green color (Submerged Plate), respectively (adapted from Massey[32]).

heating of cells in culture with the use of electromagnetic radiation.

1. MW Hyperthermia Systems

Microwaves, non-ionizing electromagnetic radiation at 30 MHz–300 GHz frequency range, can efficiently generate heat by rapid changes in the electric field within lossy media, such as cell culture samples. Recently, different types of MW applicators have been reported for *in vitro* hyperthermia assessment of cells in culture.[59–61]

Kiourti et al.[59] developed a MW system to heat the cell culture samples in a temperature controlled manner. Figure 5 shows the MW radiation system in their study that was equipped with a 2.4 GHz antenna, a 50 Ω coaxial cable to feed the antenna from the MW generator, a culture dish with copper tape to contain 2.75 mL of medium, an amplifier, and a K-type thermocouple inside the dish to record the temperature. Also, use of a 2.4 GHz sleeve balun was reported that was placed between the power amplifier output and the MW antenna input to minimize cable radiation and achieve a balanced operation.

Because of the surrounding metal shield, when the MW antenna is excited at 2.4 GHz, resonance will be achieved which will enhance heating, hence causing temperature rise within the culture dish. In their study, the generator remained 'ON' for 15 min, and the heating response was recorded as a function of time. The MW source was then turned 'OFF' to allow the medium to cool as illustrated in Fig. 5d. On average, temperature rise inside the culture dish rose from initial room temperature (24°C) to hyperthermic temperatures of 40°C and 50°C within 8 min and 15 min of MW radiation, respectively.

Temperature inside the cell culture samples can be controlled by adjusting the intensity (radiating power) and duration (exposure time) of MW radiation. Asano et al.[62] reported such system which can provide MW irradiation at varied output powers to maintain the temperature at 37°C. In their study, MW irradiation was applied at different output powers up

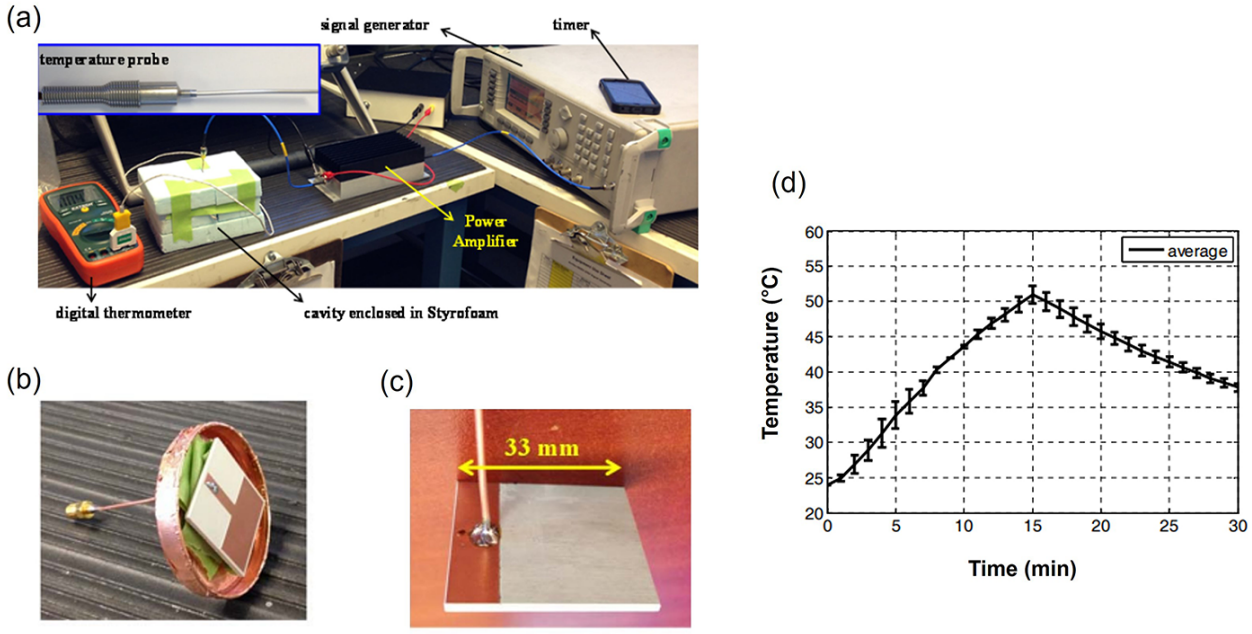

FIG. 5: MW radiation system. (a) Experimental set-up including power amplifier and a thermocouple probe connected to a thermometer for monitoring the temperature during heat exposure. (b) Proposed MW cavity for *in vitro* heating of 2.75 mL culture medium. (c) Monopole antenna to be enclosed within the MW cavity. (d) Average measured temperature of three samples with standard deviation (SD) error bars (adapted from Kiourti et al.).[59]

to 20 W to maintain the temperature under the cell culture dish at a specific value using an infrared (IR) camera. The temperature data from the IR camera was transmitted to a controller which estimates the reflected power to adjust the output power to the system radiator. According to their study, the drifting temperature over the desired temperature range was within 3°C inside the cell culture dishes (Fig. 6). The temperature ramp rate inside the cell culture media was within 1 min to achieve 37°C from initial temperature of ~ 20°C, indicating a faster ramping rate during MW heating when compared with regular incubation.

Manop et al.[61] investigated the efficacy of MW heating at cellular levels taking into account the MW power and heating time. In their study, *in vitro* MW heating experiment was performed on HepG2 cells. A MW generator was used to generate energy at the frequency of 2.45 GHz and was connected to a coaxial triple slot antenna for transferring MW energy to the target cells cultured in a 6-well plate. Fiber optic sensors were positioned within each well to measure the temperature uniformity across four different positions (Fig. 7). An IR camera was also utilized to measure the temperature at the surface of culture samples in each well. They reported the effects of different powers and heating duration on cell viability and surface temperature uniformity. Figure 7b demonstrates the temperature distribution at various points (T1–T4) inside each well during MW exposure. The heat-up phase from room temperature (~ 25°C) to target temperature was significantly reduced by increasing the power level; however, increasing the power level led to higher temperature heterogeneity (~ 5°C) throughout the sample. This indicates the trade-off between the ramping rate and temperature distribution throughout the sample.

Chen et al.[63] also performed MW irradiation to treat cancer cells. A MW needle fixed with a temperature measuring probe was inserted into

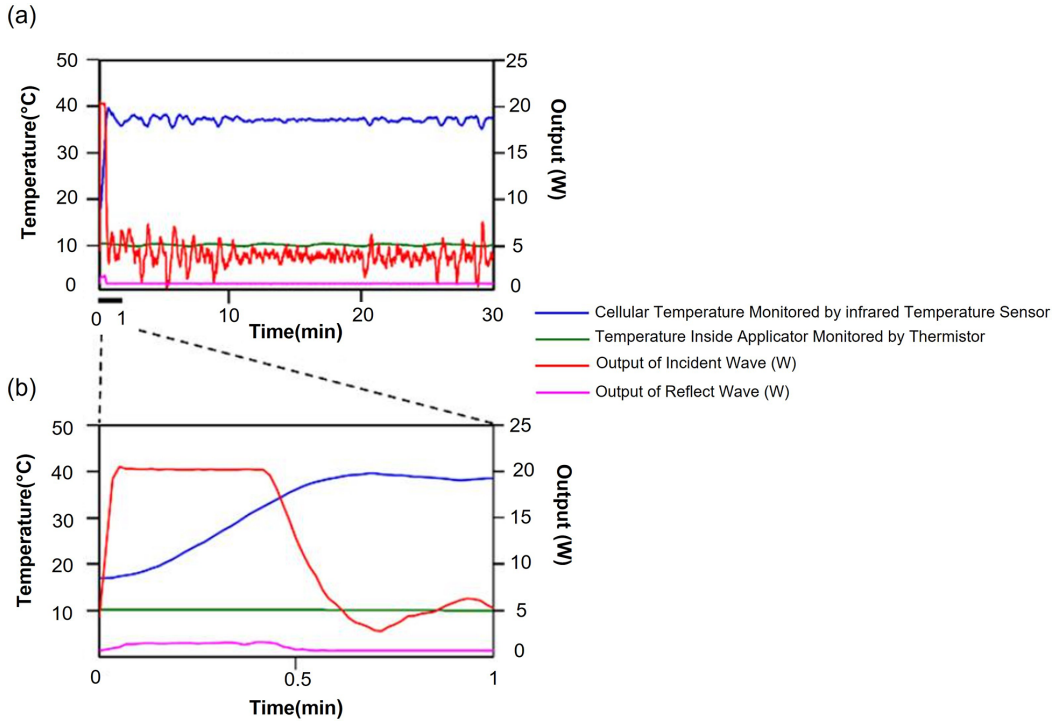

FIG. 6: Changes in temperature and output of MW irradiation. (a and b) Changes in temperature and output power within 30 min of MW irradiation (a) and over 0–1 min of MW irradiation (b). Sample temperature (shown by blue color) was monitored by an IR camera and reached the target temperature of 40°C from initial room temperature within ~ 30 s of MW irradiation, indicating a fast ramp rate (adapted from Asano et al.[62]).

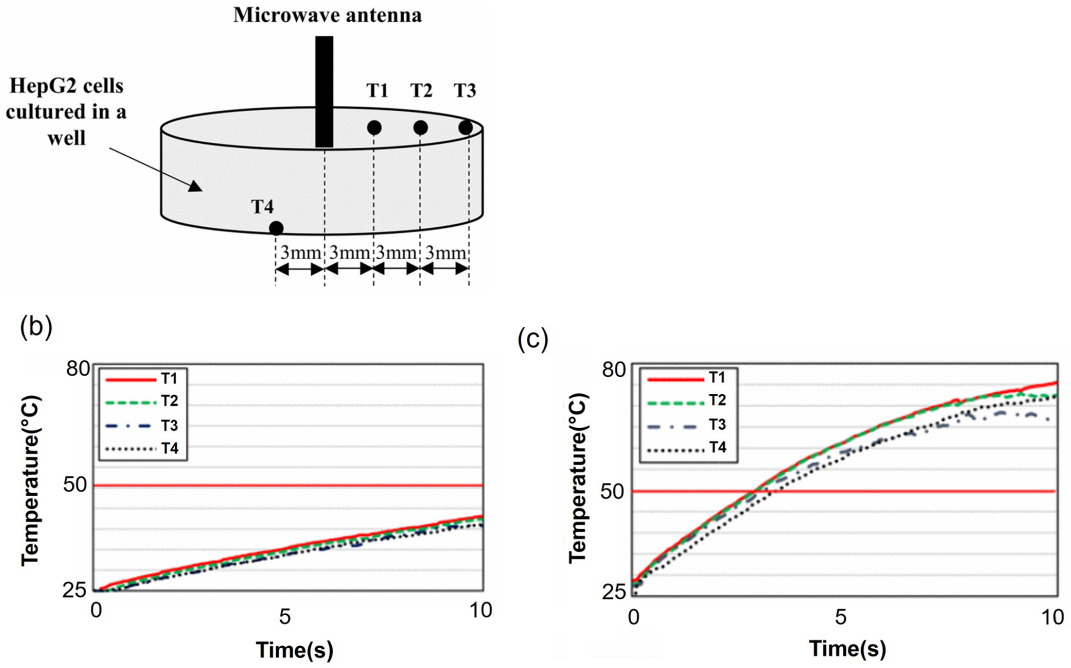

FIG. 7: (a) Placement of MW antenna and fiber optic sensors during heating experiment where all temperature sensors were placed within 3 mm spacing from each other with three sensors at the surface and one sensor at the bottom of the culture well. (b) temperature distribution at four different points during MW heating based on 5 W applied power. (c) Temperature distribution at four different points during MW heating based on 20 W applied power (adapted from Manop et al.[61]).

each well of 48-well plate containing 500 µL of cell culture media. In their study, the MW heating device was set to 15 W power. The heating duration was at 15, 20, 25, 30, 40, 50 and 60 s while the MW heating treatment was repeated 3 times for each duration. Finally, the sample temperature was recorded as depicted in Fig. 8, showing a linear relationship between sample temperature and heating duration in MW heating when using a fixed power.

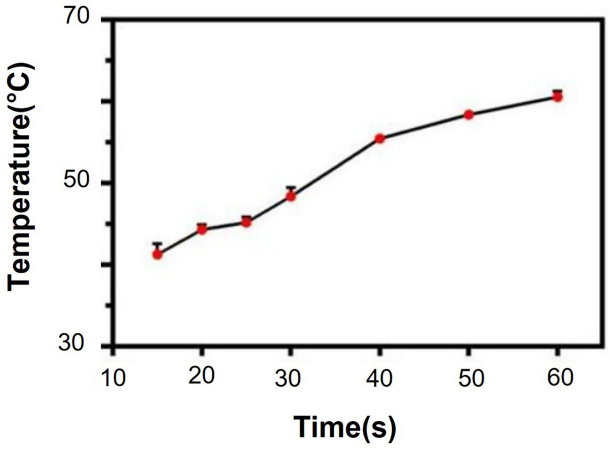

FIG. 8: Time-temperature curve based on 15 W MW heating with three trials (n = 3), indicating a linear relationship between heating time and obtained temperature. Data are expressed as the mean ± SD among multiple treatment groups. The times required to reach the target temperatures of 41, 48 and 60°C were 15, 30 and 60 s, respectively (adapted from Chen et al.[63]).

2. Near-IR (NIR) Laser

In this section, we discuss laser induced hyperthermia techniques *in vitro*, where laser illumination can produce heat in nanoscale sample volumes. The NIR laser has high penetrability and is commonly used in the treatment of lesions.[64,65] NIR laser is a form of electromagnetic radiation at wavelengths of 800–980 nm which converts optical energy into thermal energy through photo-thermal absorption.

This phenomenon leads to a rapid and direct heating inside the samples.

Inagaki et al.[66] used diode laser (810 nm) irradiation to target cells in a photocoagulation treatment. In their study, epithelial cells were seeded on 32 cm^2 culture dishes and were treated by laser irradiation. Figure 9 demonstrates their system design which includes the laser beam passing through the dichroic mirror for irradiating the cells in a culture dish.

As discussed earlier, precise control of temperature inside the samples with a uniform heating pattern and short heat-up phase are crucial to study sensitive heat-induced cellular reactions. Manderson et al.[39] reported a rapid and controlled optical heating via NIR laser incubation, where targeted illumination of a blood-antibody sample is converted into heat through photothermal absorption. In their study, a feedback control system was employed to accurately maintain the sample temperature. The heating platform included a laser incubation chamber, an NIR diode laser (980 nm), a mirror to illuminate sample mixture, and an IR temperature sensor to provide real-time temperature data to the feedback system program. Laser illumination increased the temperature of the sample volume (75 µL) from 24°C to 37°C within approximately 30 s, while the heat-up phase was approximately 150 s when using the traditional heating block technique. The fast-ramping rate in laser-based technique is due to its independence from an external heat source; instead, it is a function of laser output power which is regulated by the sample temperature. As depicted in Fig. 10, temperature control of sample was obtained via pulsating mechanism during laser-based heating with an accuracy of 1°C that was in agreement with the results presented by other groups.[67]

The laser absorption may be considered as non-uniform due to different diffusions of temperature for the seeded cells in various regions inside the culture dish, even with a fixed power. Therefore, to overcome these limitations and critical points, Miura et al.[40] developed an alternative method that allows to measure the spatial temperature distribution inside the cell culture dish while laser irradiation is being performed. Figure 11 shows the schematic view of laser irradiation platform for *in vitro* heating purposes.

As illustrated in Fig. 11a, a culture dish was placed on the heating plate to maintain 37°C prior to laser heating while the laser irradiation was being controlled by a time-controlled routine. Within seconds of laser irradiation, the temperature inside

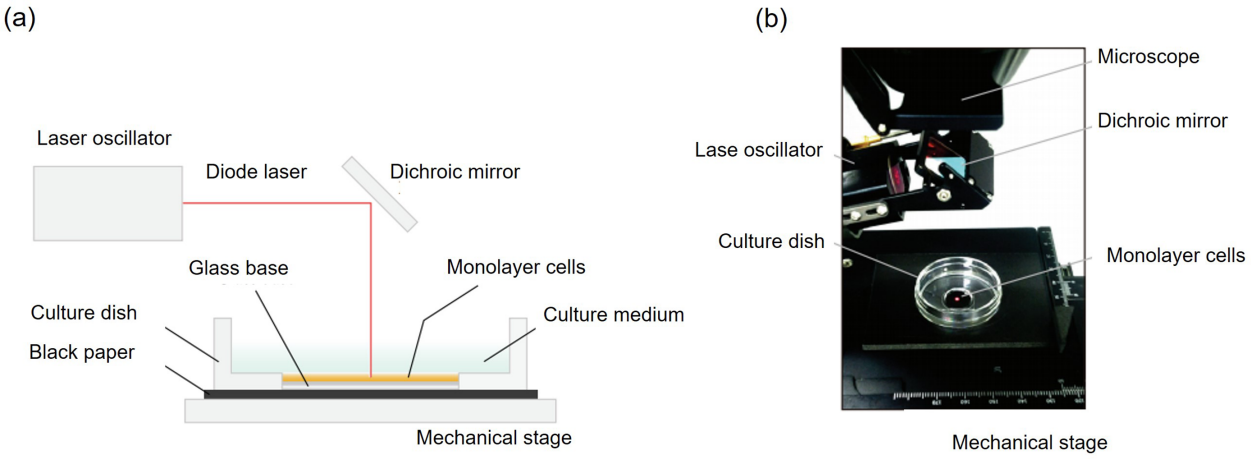

FIG. 9: Experimental setup for laser irradiation via a dichroic mirror and a perpendicular laser where cells were cultured on glass-bottomed dishes with diagram illustration (a) and photograph (b) of the experimental setup. A diode laser beam was passed through the dichroic mirror to irradiate a full confluent cultured cell layer perpendicularly on a glass-based dish. Use of culture medium with no phenol red was reported to avoid blocking diode laser light (adapted from Inagaki et al.[66]).

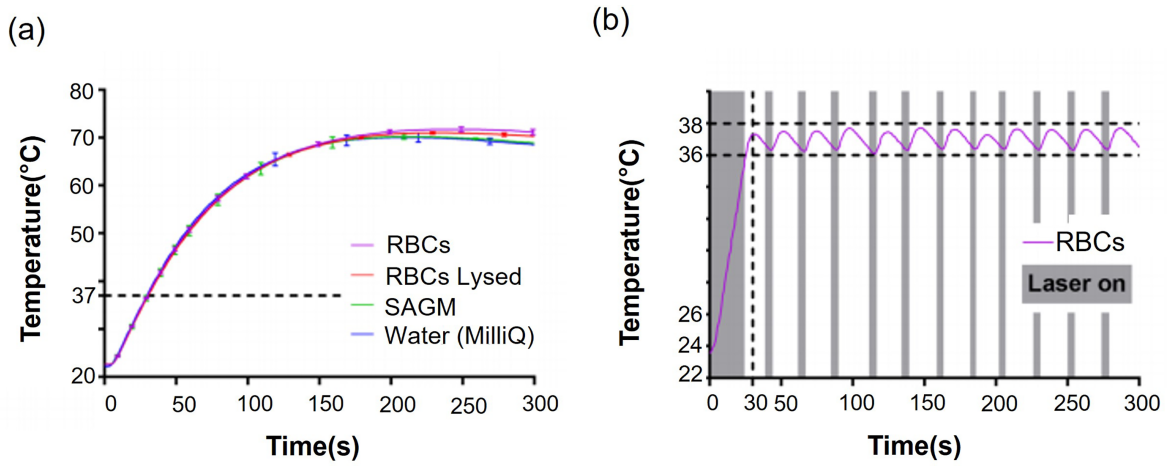

FIG. 10: Laser light absorption by red blood cells (RBCs) shown in pink color. (a) Without pulsing, laser light absorption rapidly heats the sample (75 µL) to 70°C within 150 s. (b) laser illumination with pulsed on (grey) and pulsed off (white) to maintain the sample temperature between 36°C and 38°C (adapted from Manderson et al.[39]).

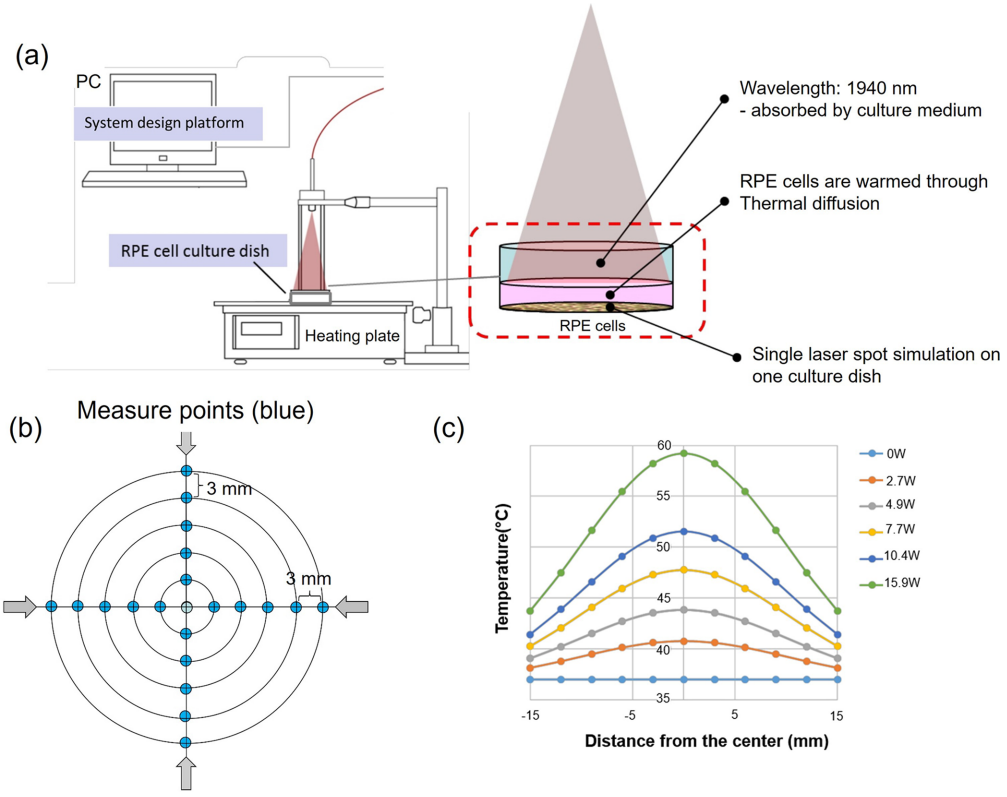

FIG. 11: (a) Schematic image of laser irradiation station consisting of a culture dish that was placed on the heating plate while the cells are placed 12 cm below the laser fiber tip for providing identical beam size to the inner diameter of the dish. (b) Measurement of the temperature distribution at 21 different positions (blue dots) inside the cell culture dish with five radial points over four different angles. (c) Non-uniform (bell-shaped) distribution of the measured temperature across the culture dish (reprinted from Miura et al. with permission from JoVE, copyright 2017[40]).

the cell culture dish increased, and led to thermal convection throughout the cells. The highlight of this study was the ability to measure the temperature distribution throughout the cell culture. The temperature distribution was created by data interpolation based on 21 points on a culture dish where fine thermocouples were inserted (Fig. 11b). Because thermocouples are not recommended to be used in sterilized cell cultures, the authors selected the same amount of medium (1.2 mL) that was used in the cell culture experiments and finally measured the temperature uniformity at the bottom of dummy (cell-free) dishes. Figure 11c highlights the center of the cell culture dish as the highest temperature that was measured during laser irradiation. Similar to previous work,[41,67] maximum measured temperature was positively correlated to laser output power. The non-uniform bell-shaped heating pattern in cell culture plates during NIR laser radiation was also reported by other groups.[68,69]

In vitro heating by laser irradiation has the advantage of a fast temperature ramping rate as well as ability of temperature control,[70] however, the drawback is that temperature is not uniformly distributed throughout the sample. One possible solution is to use lower absorption coefficient in water. However, the lasers must have high power since only a small portion of the light can be absorbed over small regions.

D. High-Intensity FUS (HIFU)

HIFU has been clinically applied to non-invasively deposit energy in deep tissues and has been used for treating several types of cancer.[71–73] Frictional heating is generated due to acoustic absorption, causing temperature rise within the sample. HIFU systems typically operate at ~ 0.5–5 MHz, providing a balance between effective heating and penetration within tissue. Although cellular response to hyperthermia treatments has been widely studied,[74,75] the underlying mechanism in which HIFU induced cellular necrosis occurs is still unclear. Zhang et al.[76] were able to design an *in vitro* based system that generates heat through ultrasound in a 96-well culture plate. The HIFU *in vitro* system (Fig. 12a) consists of a box where the transducer and culture dishes are placed. To avoid the formation of unwanted air bubble inside the culture dish, use of degassed deionized water was reported that was being circulated in the system through a water pump. Finally, a piezoelectric transducer was used in the water container to generate the ultrasound induced signal. As shown in Fig. 12b, samples were exposed to FUS at 213 W/cm^2 for 30 min. In their study, feedback loop algorithm based on real-temperature data measured by a thermal camera was reported to maintain the mean temperature of the samples at 45°C with an accuracy of ~ 2°C. A ramping rate of approximately 2 min was required to achieve a hyperthermic temperature of 45°C from 34°C.

For FUS exposures, embedding cells within cellular compatible tissue mimicking material can help to provide stability. This is because culture medium is far less attenuating than the soft tissue, causing restricted cellular heating during ultrasound exposure. Such experimental arrangement was demonstrated by Arvanitis et al.[47] In their study, the cells were embedded inside the agarose gel with glass microbeads. The cells and tissue mimicking gel were immersed in a water tank that was maintained at 37°C. A fine type-T thermocouple was inserted in the gel to record the temperature focally. The signal from the temperature sensor was recorded every 10 ms with a multiplexer, transferring the temperature data to a PC. This design however, may result in reading errors due to the possible interference between ultrasound induced beam and the thermocouple, leading to ~ 1°C temperature rise. A temperature rise of 10–25°C occurred in less than 2 s during HIFU exposures within high pressure ranges, indicating the fast ramping rate of ultrasound based heating modality. The temperature was not kept constant during the ultrasound exposure, and instead was followed with a continuous increase.

Another application stemming from the use of a HIFU was reported by Rivens et al.[45] The authors were able to embed the cells in a compressed collagen gel sandwiched between slices of PVA gel. In their study, gels were exposed to ultrasound using a transducer at 1.6 MHz frequency. A sterilized fine K-type thermocouple was vertically inserted

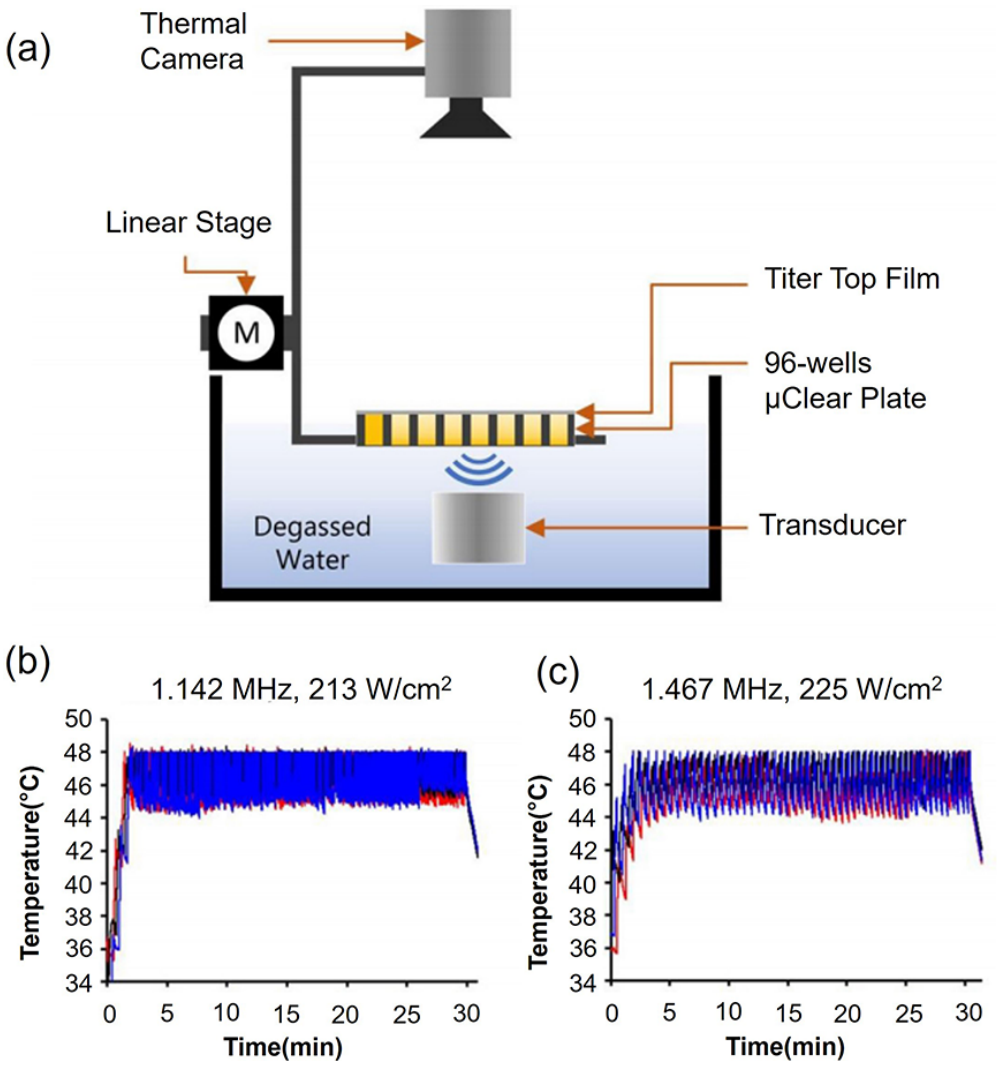

FIG. 12: The *in vitro* FUS system. (a) Diagram of experimental design where ultrasound signal was generated using a piezoelectric focused transducer driven by a signal generator that was immersed at the bottom of a tank filled with degassed water. (b) and (c) represent measured temperature during FUS exposure that was measured by an IR thermal camera at 1.142 MHz and 1.467 MHz, respectively. The red, black and blue wavy lines represent the real-time temperatures in three in-parallel sonicated waves (adapted from Zhang et al.[76]).

into the collagen layer to monitor the real-time temperature for 300 s treatment with a sampling rate of 0.01 s. An increase in the temperature of ~ 23°C was achieved within only 200 s of ultrasound exposure, confirming a fast heating rate that was in agreement with the results presented by Arvanitis et al.[47]

Although, ideally, HIFU treatment would be given as a homogeneous thermal dose distribution to all cells, this can be rarely visualized. To this end, Rivens et al.[45] measured and simulated the temperature inside the culture dish at different distances from center. As illustrated in Fig. 13a, temperature uniformity was reported within 2°C at 3 mm distance compared with center. Experimental measurements showed that heterogeneity of temperature distribution increased significantly (6°C) at distances further away from 3 mm of the

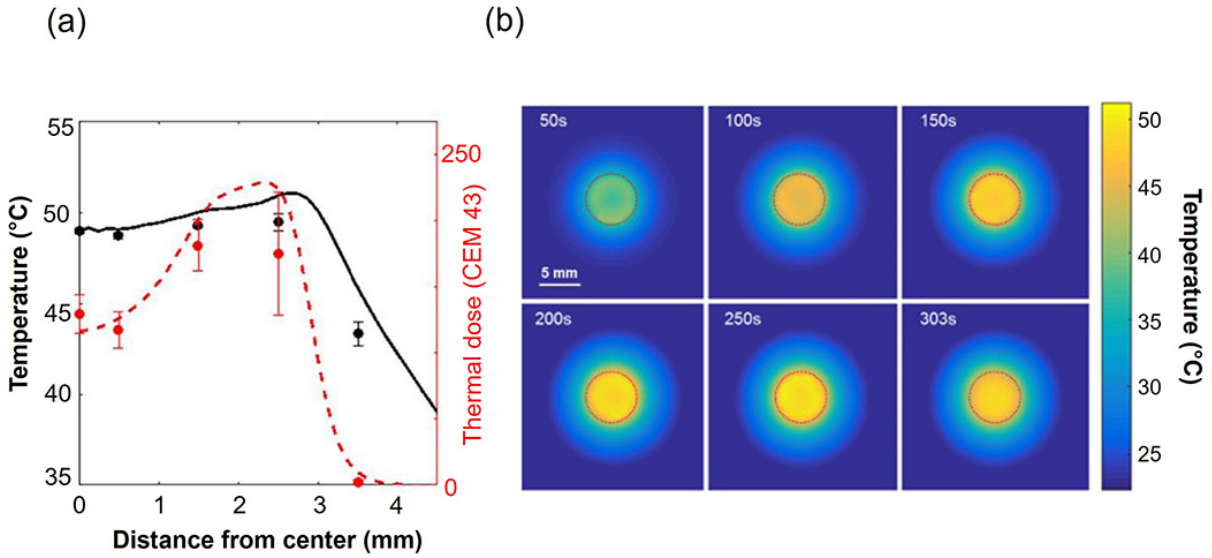

FIG. 13: Temperature distribution during ultrasound exposure throughout the collagen layer. (a and b) Comparison of simulated (solid line) and measured (markers) maximum temperature and thermal dose shown by black (temperature) and red (thermal dose), respectively (a) and simulated temperature distributions at different time points ranging from 50 s to 300 s (b) (adapted from Brüningk et al.[45]).

center. Therefore, achieving a uniform heating pattern during HIFU exposures might be difficult, supporting the simulation results depicted in Fig. 13b.

To allow long-term cellular manipulation, it is necessary to maintain a stable temperature. Manneberg et al.[46] were able to integrate an ultrasonic heating system using a microplate. In their study, temperature dependency on applied voltage was obtained by inserting a probe in each well of the microplate as illustrated in Fig. 14. In their study, the heat-up phase was ~ 20 min to stabilize the temperature of the ultrasonic device. Following the stabilization, the temperature was maintained stable over a long period of 15 hours with a high degree of accuracy (standard deviation of 0.02°C). The uniformity of temperature was also measured over the chip surface (from the transducer to the opposite corner of the chip) that was within 1°C, estimated to cause ~ 0.3°C difference in temperature uniformity throughout the samples. The presented heating technique by Manneberg et al.[46] enables precise temperature control with high degree of accuracy and uniformity throughout the samples; however, the temperature ramp rate is very slow (0.2–2°C min^{-1}), indicating a major drawback of this heating modality.

E. Microheating Plates

Several heating modalities using microheaters have been reported for cell culture studies. These methods utilize heating elements and cell culture chambers to establish a controlled heating throughout the living cells. Heating elements used in microheaters are not only electrically conductive but also optically transparent, and Joule heating can be generated when electrical power is applied. Mäki et al.[77] designed such microheater system with a temperature control working principle using a proportional-integral derivative controller. In their study, they utilized an indium tin oxide plate as a heating element (70 × 70 × 0.7 mm), a temperature sensor made on a glass substrate (49 × 49 × 1 mm), a cell culture chamber, and a custom-written MATLAB (MathWorks, Inc., Natick, MA, USA) user interface software for controlling the temperature (Fig. 15). Temperature measurement was performed by using 14 identical sensors that were attached on the heating plate. The set power of the controller was limited to 2 W.

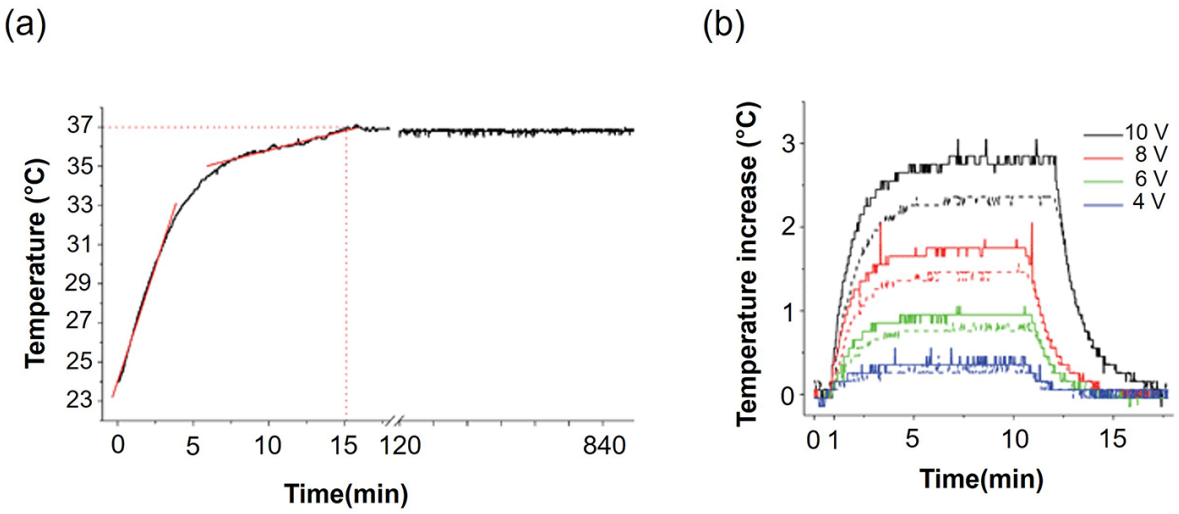

FIG. 14: Temperature control during ultrasound heating. (a) Temperature calibration and maintenance at 37°C where red lines show the approximate rates of the faster ultrasonic and slower chamber heating. (b) Temperature was measured adjacent to the transducer (solid lines) that was dependent on the applied voltage (4−10 V) over the transducer and within the fluid in the micro-wells (dotted lines) (reprinted from Vanherberghen et al. with permission from The Royal Society of Chemistry, copyright 2010[46]).

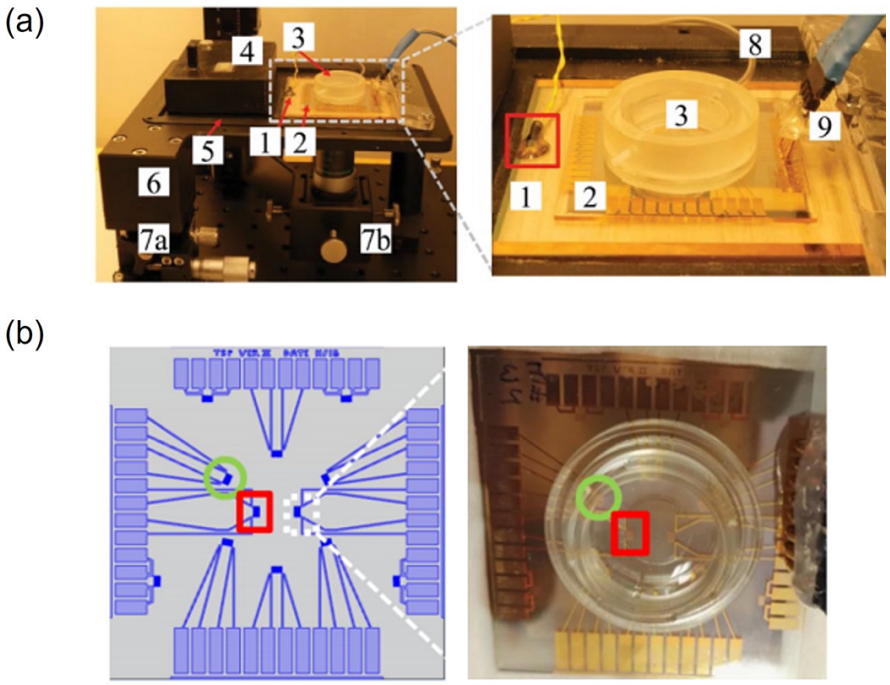

FIG. 15: Microscale cell culture system. (a) Experimental setup consisting of ITO plate as the main heating component, a temperature sensor plate made on glass substrate and a cell culture device. (b) Temperature logging designed sensor layout and temperature sensor plate together with cell culture chamber. Sensor is marked with a green circle while resistors are marked with a red square (reprinted from Mäki et al. with permission from SAGE, copyright 2022[77]).

This microscale cell culture system precisely controls cell culture temperature with an accuracy of ~ 0.3°C during heating, as shown in Fig. 16a. This was similar to that in other studies; for instance, temperature variations of ± 0.2°C,[78–80] ± 0.26°C,[81] ± 0.3°C,[82] ± 0.5°C,[83] and ± 0.8°C[84] have been previously measured.

Despite an accurate control of temperature during heating, the system still lacks some of the requirements for an ideal heating modality. The heat-up phase took ~ 20 min to reach to the target temperature of 37°C from initial room temperature of 24°C (Fig. 16b). Moreover, temperature uniformity was measured between the min and max values over the cell culture area by using a thermal camera, and was reported as ± 2°C.

Lin et al.[79] developed an indium tin oxide (ITO)-based microheater chip that serves as a thermal control system for perfusion cell culture outside the incubator. The device consists of a multi-channel syringe pump for media supply, medium feeding tubing, microcontroller, perfusion micro-bioreactor chambers with the format of a standard 96 well cell culture microplate each containing 50 µl of the mixture, ITO microheater chip, thermocouple, and medium outlet tubing. Figure 17a shows the

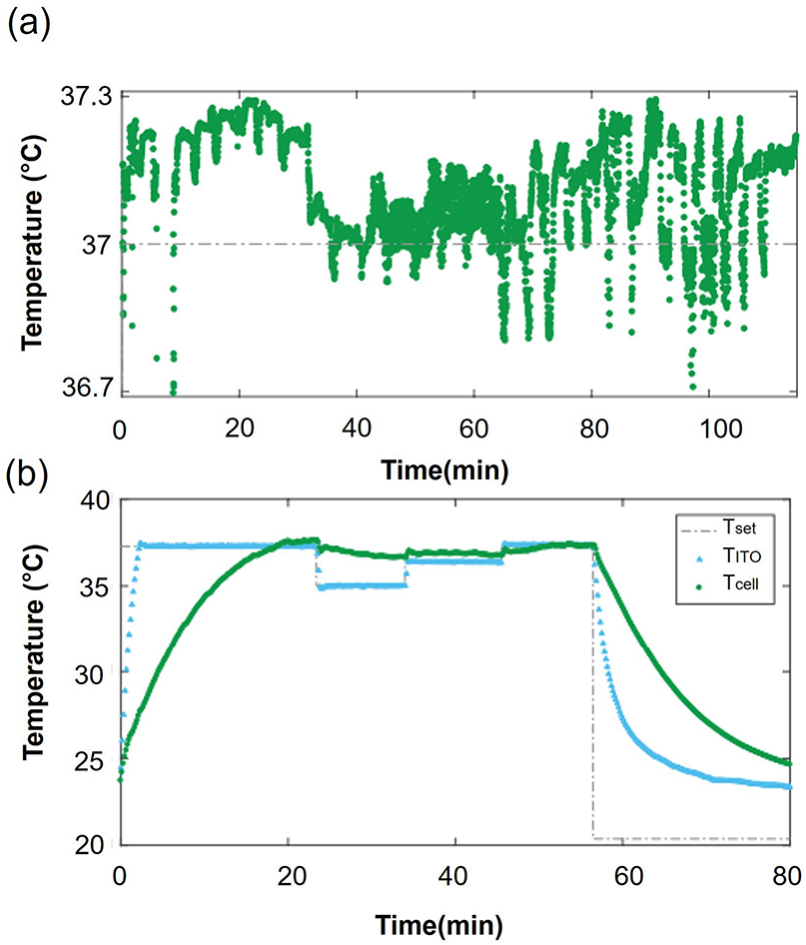

FIG. 16: Temperature control. (a) Long-term maintenance of the cell culture temperature with 0.3°C accuracy for more than 4 days. (b) Measured cell culture temperature during heating experiment where the set-point temperature was randomly changed, and both $T_{outside}$ and T_{cell} were recorded (reprinted from from Mäki et al. with permission from SAGE, copyright 2022[77]).

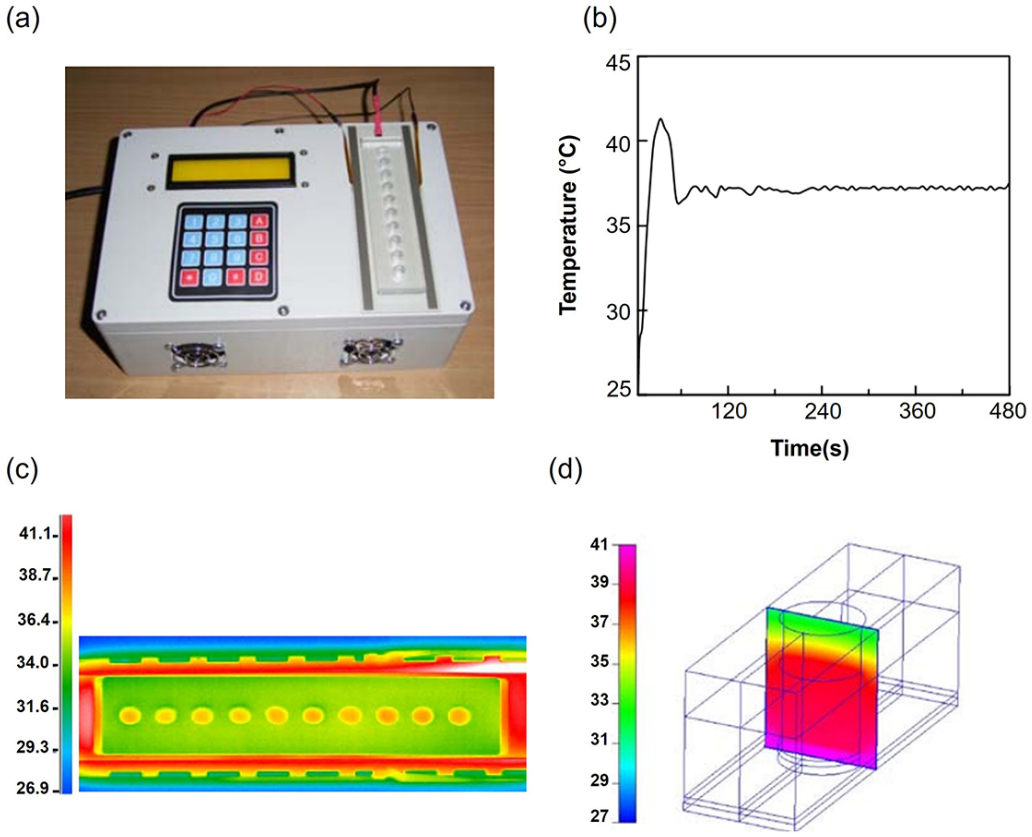

FIG. 17: Temperature control. (a) Photograph of the handheld microcontroller (17.1 cm × 11.6 cm × 6.5 cm) with an ITO microheater chip connected and a perfusion block. (b) Temperature profile over time (the set temperature was 37°C and the temperature deviation was evaluated to be within 0.2°C. (c) Two-dimensional IR images of top surface of ITO microheater chip and chambers. (d) Numerical simulation based temperature evaluation inside the polydimethylsiloxane microbioreactor chamber (reprinted from Nieto et al. with permission from Elsevier, copyright 2017[79]).

microcontroller module with the ITO microheater chip designed in this study.

The thermal control mechanism is based on a feedback control loop. In their study, a thermocouple was used to monitor the local temperature over the sample where the thermal field needs to be closely regulated. Then, the generated temperature profile was inputted to the microcontroller module to constantly adjust the output electric current and maintain the temperature. The accuracy of temperature control was experimentally measured as shown in Fig. 17b, indicating high degree of temperature control with slight deviation of ± 0.2°C following the heat-up phase. The heat-up phase was reasonable short (~ 60 s) to reach the target temperature of 37°C from initial room temperature of ~ 26°C. Temperature distribution uniformity over the culture samples was evaluated by numerical simulation and experimental evaluation. Experimental evaluation was carried out by IR imaging after filling each micro-bioreactor chamber with cell culture medium. IR imaging demonstrated that a uniform thermal field can be obtained at the top surface of each micro-bioreactor chamber with slight variation of ± 0.2°C as shown in Fig. 17c. Despite the uniformity of temperature distribution at the top surfaces, simulation results revealed that uniform temperature distribution could not be achieved vertically (bottom to top variation) inside each chamber. Figure 17d indicates a non-uniform vertical temperature distribution in one chamber with variations higher than 5°C. Another drawback of this microheater system is

temperature overshooting (~ 4°C higher than the target temperature) during the heat-up phase as shown in Fig. 17b. This is a major disadvantage since large variations at hyperthermic temperatures can significantly affect the cellular/molecular response even within short periods.

Petronis et al.[81] also presented a cell culture chip integrated with indium-tin-oxide heater to provide steady and spatially uniform thermal conditions using a proportional-integral derivative feedback control system. The software adjusted the voltage (2.2–2.9 V) applied to the heater based on the temperature readings to maintain the temperature of the cell culture. The cell culture chip was composed of five poly (methyl methacrylate) sheets, cell culture chamber (7.6 × 13.0 mm^2) with inlet and outlet media perfusion, and a thermistor connected to the computer and the external power source for temperature control. In their study, the microheater was tested for thermal control stability and they reported an accurate control of temperature with slight variation (± 0.26°C). Similar to Lin et al.,[79] the simulation based analysis was performed to evaluate the temperature distribution uniformity throughout the cell culture chamber. Results of 2-D temperature distribution modeling indicate heterogeneity up to 3°C along the cell culture chamber during a steady state heating of 37°C.

Recently, Nieto et al.[83] reported fabrication of a glass based microheater (5 × 5 mm^2) that was comparable to conventional cell incubators for cell culture in terms of temperature rise and decay characteristics and localized heating. Thermal characterization of the microheater was measured by an IR Camera that was placed over the microheater to record the local temperature when the microheater was subjected to different applied voltages (Fig. 18a). There was no measurement regarding the temperature ramp rate or the accuracy of temperature control inside the cell culture chamber. The main weakness of their experimental measurements was that only the response characteristics of the microheater chip was measured and not the cell culture chamber. Temperature distribution throughout both the cell culture chamber and the microheater was captured by an IR camera which can be visualized in Fig. 18b. Regions near the microheater chip demonstrate higher temperatures compared with regions further away from the microheater chip, indicating a non-uniform temperature distribution (~ 10°C variation) inside the whole cell culture chamber. One reason for this heterogeneity could be due to the large size (2 mm in depth and 8 mm in diameter with the total volume of 900 μL) of cell culture chamber compared with regular 96-well plates that are supplied with less volume (~ 200 μL per well) of cell culture media.

F. Microfluidic Systems

Microfluidic systems are those that employ devices for processing and manipulation of small fluid volumes (10^{-9}–10^{-18} L) within fabricated systems. These systems consist of a series of generic components: a method for introducing fluidic samples; methods for moving the samples around on the microfluidic chip, a method for combining and mixing; and various other devices such as cell carrier, heating elements, and syringe pump.[85] Several biological applications have been reported using microfluidic devices. While they have not been widely used in hyperthermia research, microfluidic systems offer experimental flexibility to culture cells within a controlled environment.[86,87] Approaches to accurately control the temperature within microfluidic systems have been already proposed. Accurate zonal heating in microfluidic systems may be achieved through using complex on-chip resistive heater networks which requires additional fabrication steps.[88] Conversely, non-zonal heating can be achieved by using a Peltier device.[89]

De Mello et al.[90] showed controlled heating (± 0.2°C) of the sample medium near electrodes within a cell culture chamber using an alternating current (50 Hz). However, precise control of heating for large variations of temperatures remains difficult. Moreover, this method did not lead to temperature uniformity due to boundary effects.

Burke et al.[91] used a millifluidic device to quantify the content of released liposomes following mild hyperthermia. Their system consisted of a quartz capillary tube which was anchored on top of the Peltier heating elements while was attached to a syringe pump as demonstrated in Fig. 19a. In their study, the

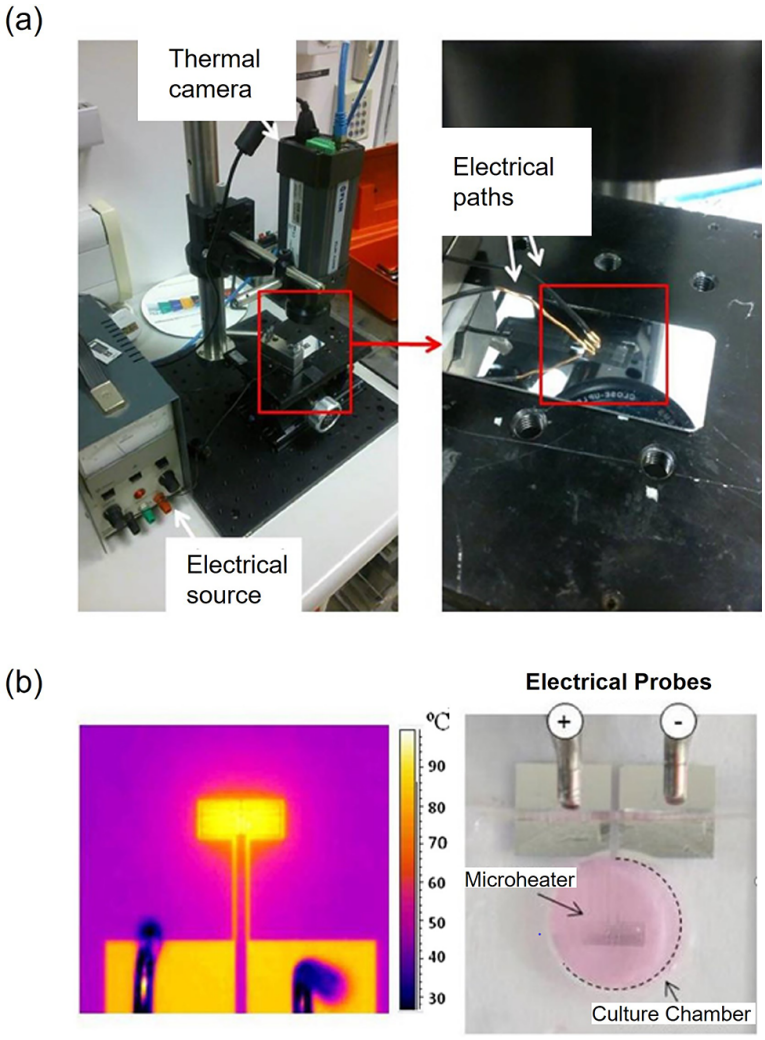

FIG. 18: Experimental setup for IR camera setup used for analyzing the heating capabilities of the microheaters and an IR image of the microheater including a detailed view of microheater and electrical connectors (a) and an IR image of the microheater obtained by the thermal camera during heating as well as top view of culture chamber used for performing cell culture (b). The bright spot on the ablation area of the microheater shows the peak temperature of 100°C (adapted from Nieto et al.[83]).

output power was adjusted to the Peltier elements to control the temperature. This was done through a feedback loop based on thermocouple temperature readings. Feedback thermocouples were placed in the water reservoir and inside the tube 8mm from the outflow.

The developed millifluidic system enabled quantification of content release of liposomes affected by mild hyperthermia at very high temporal resolution of less than 1 s. Figure 19b shows the measured temperature of the fluid entering the capillary tube that reached the desired hyperthermic temperature of 43°C within 3 mm, corresponding to 0.3 s at a flow velocity of 10 mm/s. As demonstrated, temperature control was performed with an accuracy of ~ 1°C during hyperthermia exposure. To investigate the temperature uniformity, point measurements were made throughout the surface of the heating element. Heating uniformity at the surface of Peltier element was within 2°C. Thus, to improve

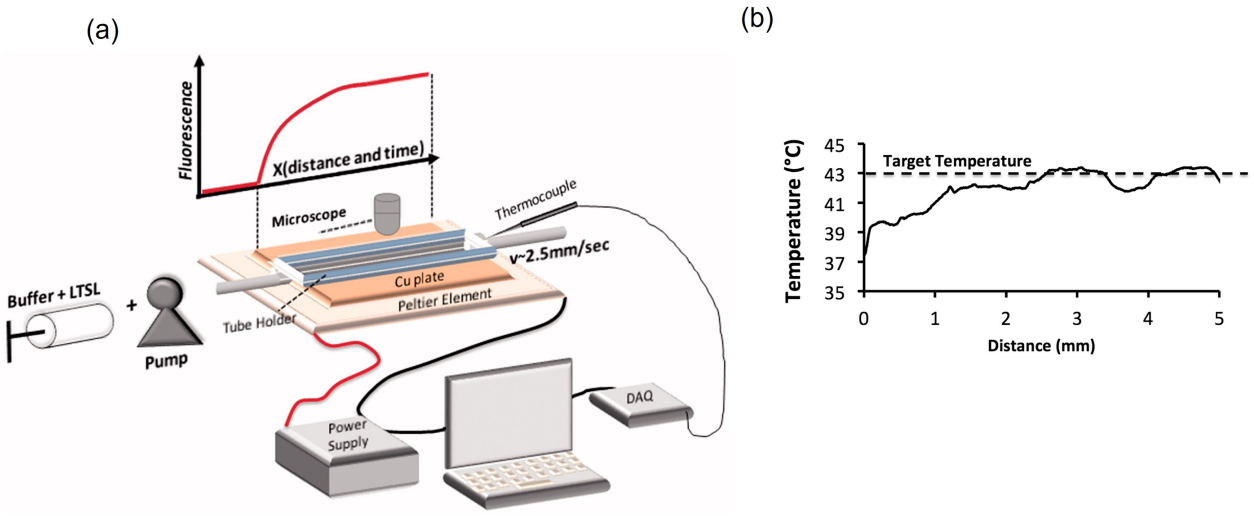

FIG. 19: (a) Schematic of experimental setup for millifluidic release assay. The tube was heated to the desired hyperthermic temperature through a temperature-controlled Peltier element. (b) Fluid entering the capillary tube reached the desired temperature within 3 mm, corresponding to 0.3 s. The Peltier temperature is measured by a thermocouple and a control algorithm regulates the output power to control the temperature (reprinted from Burke et al. with permission from Taylor & Francis, copyright 2018, http://www.tandfonline.com[91]).

this, use of a thin copper layer was reported that was secured on top of the element. This resulted in improved heating uniformity from 2°C to 0.5°C.

Cantoni et al.[92] also reported use of a flexible microfluidic device with temperature control ability for biomedical applications. In their study, Eppendorf tubes (0.5−5 mL) can be inserted into the carrier according to experimental needs (Fig. 20a). The carrier consisted of an integrated perfusion system to recirculate the culture media by using piezo pumps while a thermocouple was placed against the heater to provide temperature control feedback. Stable temperature control at 37°C with ~ 0.2°C accuracy was obtained by placing a thin heating layer under the chip. Temperature uniformity along the channel was investigated by using an IR camera (Fig. 20b). A temperature gradient of ~ 0.5°C was detected at the inlet and the center of the chip for 30 s when a flow of 50 µl/min was applied. Similar to Burke et al.,[91] one of the limitation of this study was inability to measure the sample temperature distribution. Although the temperature uniformity was monitored at the surface of the heating element, there was no report of actual cell culture sample uniformity during heating phase.

Microfluidics enables the precise application of experimental conditions to study the behavior of cells. The advantages of microfluidic cell culture over the macro-scale methods include fast ramping rate (i.e. less than 1 s), reduced risk of contamination, design flexibility and most importantly, ability to provide cell's natural microenvironment. Although microfluidic devises can provide great flexibility with respect to experimental design, transferring cells from a macroscopic culture environment of flasks, dishes and well-plates to microfluidic cell culture requires revision of culture protocols, and thus increased complexity of the system. Furthermore, variation of velocity across the tube diameter may increase systemic error as described by Burke et al.[91] Another error source in these systems could arise from photobleaching phenomenon which significantly limits the heat exposures duration of cell culture samples.[91,93]

III. COMPARATIVE ANALYSIS

In vitro studies with high degree of control of thermal profiles within cells in culture have been essential for understanding the relationship between

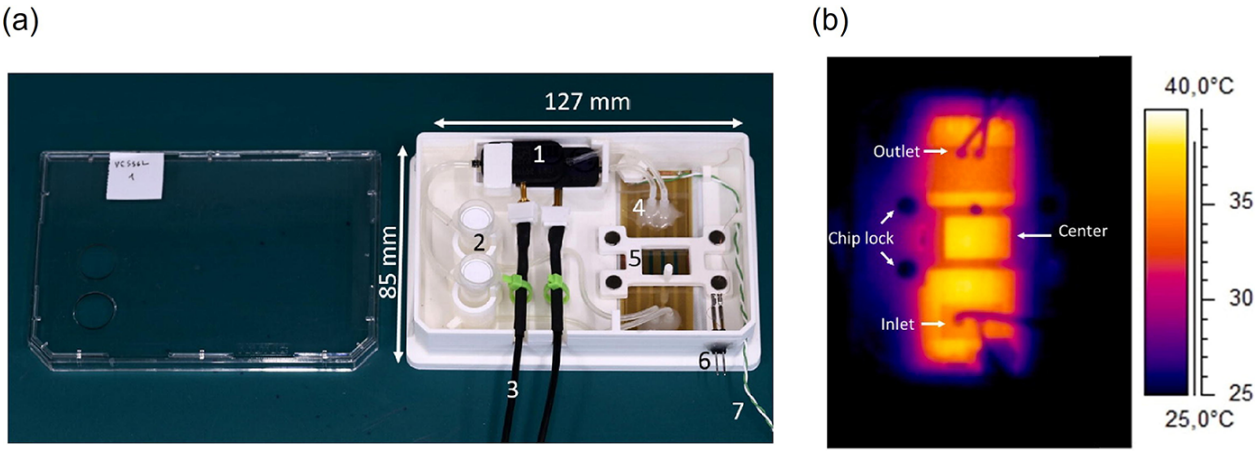

FIG. 20: (a) Microfluidic chip on the carrier consisting of piezo pumps, cell media reservoirs and the pump connectors and the thermocouple. Each pump is connected to an Eppendorf tube placed vertically inside the carrier which acts as a cell media reservoir. (b) Temperature distribution measured by IR camera after the recovery of the cell media turnover inside the microfluidic chip. Figure reproduced from (Catani et al.) under a Creative Commons license.

bioeffects and applied thermal doses. To perform an accurate analysis, cell culture samples would ideally be subjected to uniform heating, raised from, and returned to, baseline rapidly following addition/removal of the thermal source, for a known heating duration under ideal isothermal condition. The present article has surveyed a variety of heating modalities that have been used for *in vitro* studies investigating bioeffects of heating. These techniques offer different advantages or drawbacks in terms of integration and control over heating parameters such as ramp rate, accuracy, uniformity, and ease of use that are summarized in Table 1.

A. Heating Accuracy

While most heating modalities have been suitable for delivering the heat in a temperature-controlled manner, the control over thermal parameters varies considerably. Use of water baths lead to stable heating with relatively small variations (± 0.3°C) over the heating period while other heating modalities using electromagnetic waves such as MW and lasers irradiations are associated with larger variations (0.8–4°C) in terms of temperature stability. This is a drawback of using MWs, lasers and also traditional cell culture incubators since even slight temperature variations (± 0.5°C) during long treatments periods can significantly affect cellular response,[74,94] causing inaccurate *in vitro* thermal analysis.

B. Ramp Rate

The heating rate in conventional water baths and CO_2 incubators is very slow, requiring a long heat-up period (80–2400 s) to reach the desired hyperthermic temperatures (42–50°C), hence it will be difficult to obtain a detailed thermal history (i.e., temperature × time) at cellular levels using these traditional techniques. On the other hand, more integrated heating modalities including MW, laser, FUS, and microfluidic systems can achieve fast temperature ramp rates ranging from 0.1 to 10°C/s, indicating their major advantage over traditional heating techniques. The slow temperature ramp rate in water bath heating modalities can be significantly improved by incorporating a number of modifications in the system design as follows.

Use of hot media exchange technique during the transition phase and prior to immersion in water bath results in an ideally quick heat-up period (~ 5 s) to reach the target temperature as described by Rylander et al.[57] and Herea et al.[31] Unfortunately, this heating approach necessitates the use of large

sample volumes (~ 70 mL) while use of smaller sample volumes such as 96-well plates will not be practical. This is because each of the wells in a 96-well plate usually contain small volumes (100–200 μL) of cell culture sample, thus in well temperature may drop quickly within few seconds following injection and prior to immersion in preheated water bath. Heating larger sample volumes tend to show less uniformity and/or accuracy during heating phase, so the proposed approach may have its own drawbacks despite its major advantage. Conversely, use of very small volumes (in the scale of microliters) leads to instant temperature drop and inaccuracy of temperature control during heating.[58]

Another technique that can be used to compensate for the slow temperature ramp rate during water bath heating is using multiple water baths in the treatment design: One water bath set to a significantly higher temperature (e.g., 80°C) than the target hyperthermic temperature (42–50°C), to be used during the transition phase, and one water bath set to target hyperthermic temperature to be used during steady-heating phase. This heating technique, however may introduce a complexity to the heating platform since switching the culture samples from first water bath to the second one must be performed in exact timing to avoid further temperature rise of the samples above the target hyperthermic temperature.[95]

C. Heating Uniformity

Another characteristic that has been emphasized by several authors is uniformity of temperature distribution during hyperthermia exposures.[40,47,96–98] Using 96-well plate formats is ideal for subjecting cells to uniform heating due to the small sample volume (100–200 μL) in each well. Water baths and cell culture CO_2 incubators can be easily integrated with 96-well plates, resulting in ideal uniform heating inside each well. Unfortunately, most newly developed *in vitro* heating modalities including MW, FUS, laser, microheaters, and microfluidic devices involve the use of large sample volumes (e.g., T75 culture flasks, six-well plates, 30-mm petri dishes, beakers, or agar gels) due to technical limitations of the design. This can lead to higher variations (2–5°C) in temperature distribution during heating. Therefore, level of complexity is not necessarily a determining factor in selecting ideal *in vitro* heating modalities.

D. Consideration of Non-Thermal Impacts of *In Vitro* Hyperthermia Instrumentation

An ideal *in vitro* heating modality should not affect the cellular/molecular activity if used under normothermic (36.5–37.5°C) conditions. This is to ensure that the resulted change in cellular/molecular behavior can be solely attributed to the heat effects; otherwise, inaccurate thermal analysis may be made. Recently, Asano et al.[62] reported decreased cell viability following subjecting cultured cells to normothermic conditioned MW irradiation (37°C for 1 h), indicating that MW irradiation may not be an ideal *in vitro* heating modality for studying the thermal dose dependency of cell viability. Similarly, use of conventional water baths may affect cell viability even at normothermic temperatures,[29] but this is possibly due to biological contamination, hence careful handling and sufficient sealing need to be performed during the hyperthermia exposure of cell culture samples. There was no change in viability of the cultured cells that were exposed to very low doses of laser irradiation;[40] however, other physiological changes were reported such as overexpression of heat shock proteins,[99,100] this may result in inaccurate analysis between hyperthermia induced cell viability and protein expression kinetics when using laser irradiation as the heating modality. Moreover, there have been reports of artifacts and induced cell death arising from a chemical interaction between cell culture samples and polydimethylsiloxane formulations, which are commonly used in microfluidic cell culture devices.[86,101]

All heating modalities discussed in the present review were carried out on two-dimensional (2D) cultured cells. Currently, evidence suggests that cells cultured in 2D conditions may not be ideal representation of the cells existing in complex tissue microenvironments. Song et al.[102] highlighted the importance of selecting three-dimensional (3D) cell culture models in assessing cellular responses to hyperthermia treatment. Currently, there are limited number of published studies focusing on

hyperthermia-induced cellular response where the cells are cultured in 3D conditions.

ACKNOWLEDGMENT

We gratefully acknowledge support from the National Institutes of Health through Grant R01EB028848.

REFERENCES

1. Dewey WC. Arrhenius relationships from the molecule and cell to the clinic. Int J Hyperthermia. 2009;25(1):3–20.
2. Song CW, Shakil A, Osborn JL, Iwata K. Tumour oxygenation is increased by hyperthermia at mild temperatures. 1996. Int J Hyperthermia. 2009;25(2):91–5.
3. Vujaskovic Z, Poulson JM, Gaskin AA, Thrall DE, Page RL, Charles HC, MacFall JR, Brizel DM, Mayer RE, Prescott DM, Samulski TV, Dewhirst MW. Temperature-dependent changes in physiologic parameters of spontaneous canine soft tissue sarcomas after combined radiotherapy and hyperthermia treatment. Int J Radiat Oncol Biol Phys. 2000;46(1):179–85.
4. Tashjian JA, Dewhirst MW, Needham D, Viglianti BL. Rationale for and measurement of liposomal drug delivery with hyperthermia using non-invasive imaging techniques. Int J Hyperthermia. 2008;24(1):79–90.
5. Li L, ten Hagen TLM, Bolkestein M, Gasselhuber A, Yatvin J, van Rhoon GC, Eggermont AMM, Haemmerich D, Koning GA. Improved intratumoral nanoparticle extravasation and penetration by mild hyperthermia. J Control Release. 2013;167(2):130–7.
6. Li CY, Dewhirst MW. Hyperthermia-regulated immunogene therapy. Int J Hyperthermia. 2002;18(6):586–96.
7. Nomikou N, McHale AP. Microbubble-enhanced ultrasound-mediated gene transfer-towards the development of targeted gene therapy for cancer. Int J Hyperthermia. 2012;28(4):300–10.
8. Frey B, Weiss EM, Rubner Y, Wunderlich R, Ott OJ, Sauer R, Fietkau R, Gaipl US. Old and new facts about hyperthermia-induced modulations of the immune system. Int J Hyperthermia. 2012;28(6):528–42.
9. Schildkopf P, Ott OJ, Frey B, Wadepohl M, Sauer R, Fietkau R, Gaipl US. Biological rationales and clinical applications of temperature controlled hyperthermia-implications for multimodal cancer treatments. Curr Med Chem. 2010;17(27):3045–57.
10. Zhang HG, Mehta K, Cohen P, Guha C. Hyperthermia on immune regulation: A temperature's story. Cancer Lett. 2008;271(2):191–204.
11. Oei AL, Vriend LEM, Crezee J, Franken NAP, Krawczyk PM. Effects of hyperthermia on DNA repair pathways: One treatment to inhibit them all. Radiat Oncol. 2015;10(1):165.
12. Armour EP, Wang ZH, Corry PM, Martinez A. Sensitization of rat 9L gliosarcoma cells to low dose rate irradiation by long duration 41 degrees C hyperthermia. Cancer Res. 1991;51(12):3088–95.
13. Jones EL, Vujaskovic Z, Craciunescu O, Prosnitz LR, Havrilesky L, Secord A, Stauffer P, Dewhirst MW. International phase III trial of chemoradiotherapy ± hyperthermia for locally advanced cervix cancer: Interim update on toxicities. Int. J Radiat Oncol Biol Phys. 2007 Nov 1;69(3 Suppl 1):S392–3.
14. Sneed PK, Stauffer PR, McDermott MW, Diederich CJ, Lamborn KR, Prados MD, Chang S, Weaver KA, Spry L, Malec MK, Lamb SA, Voss B, Davis RL, Wara WM, Larson DA, Phillips TL, Gutin PH. Survival benefit of hyperthermia in a prospective randomized trial of brachytherapy boost +/– hyperthermia for glioblastoma multiforme. Int J Radiat Oncol Biol Phys. 1998;40(2):287–95.
15. Issels RD, Lindner LH, Verweij J, Wust P, Reichardt P, Schem BC, Rahman S, Daugaard S, Salat C, Wendtner CM, Vujaskovic Z, Wessalowski R, Jauch KW, Durr HR, Ploner F, Melnyk AB, Mansmann U, Hiddemann W, Blay JY, Hohenberger P. Neo-adjuvant chemotherapy alone or with regional hyperthermia for localised high-risk soft-tissue sarcoma: A randomised phase 3 multicentre study. Lancet Oncol. 2010;11(6):561–70.
16. Knab LM, Salem R, Mahvi DM. Minimally invasive therapies for hepatic malignancy. Curr Probl Surg. 2013;50(4):146–79.
17. Ahmed M, Brace CL, Lee FT, Goldberg SN. Principles of and advances in percutaneous ablation. Radiology. 2011;258(2):351–69.
18. Chu KF, Dupuy DE. Thermal ablation of tumours: Biological mechanisms and advances in therapy. Nat Rev Cancer. 2014;14(3):199–208.
19. Markezana A, Ahmed M, Kumar G, Zorde-Khvalevsky E, Rozenblum N, Galun E, Goldberg SN. Moderate hyperthermic heating encountered during thermal ablation increases tumor cell activity. Int J Hypothermia. 2020;37(1):119–29.
20. Gasselhuber A, Dreher MR, Rattay F, Wood BJ, Haemmerich D. Comparison of conventional chemotherapy, stealth liposomes and temperature-sensitive liposomes in a mathematical model. PLoS One. 2012;7(10):e47453.
21. Gameiro SR, Higgins JP, Dreher MR, Woods DL, Reddy G, Wood BJ, Guha C, Hodge JW. Combination therapy with local radiofrequency ablation and systemic vaccine enhances antitumor immunity and mediates local and distal tumor regression. PLoS One. 2013;8(7):e70417.
22. Haen SP, Pereira PL, Salih HR, Rammensee HG, Gouttefangeas C. More than just tumor destruction: Immunomodulation by thermal ablation of cancer. Clin Dev Immunol. 2011;2011:160250.
23. Dewhirst MW, Vujaskovic Z, Jones E, Thrall D. Re-setting the biologic rationale for thermal therapy. Int J Hyperthermia. 2005;21(8):779–90.

24. Hildebrandt B, Wust P, Ahlers O, Dieing A, Sreenivasa G, Kerner T, Felix R, Riess H. The cellular and molecular basis of hyperthermia. Crit Rev Oncol Hematol. 2002;43(1):33–56.
25. Tang Y, Lei T, Manchanda R, Nagesetti A, Fernandez-Fernandez A, Srinivasan S, McGoron AJ. Simultaneous delivery of chemotherapeutic and thermal-optical agents to cancer cells by a polymeric (PLGA) nanocarrier: An in vitro study. Pharm Res. 2010;27(10):2242–53.
26. Dewey WC. Arrhenius relationships from the molecule and cell to the clinic. Int J Hypothermia. 2009;25(1):3–20.
27. Tang Y, McGoron AJ. Combined effects of laser-ICG photothermotherapy and doxorubicin chemotherapy on ovarian cancer cells. J Photochem Photobiol B. 2009;97(3):138–44.
28. Rong Y, Mack P. Apoptosis induced by hyperthermia in Dunn osteosarcoma cell line in vitro. Int J Hypothermia. 2000;16(1):19–27.
29. Shellman YG, Ribble D, Yi M, Pacheco T, Hensley M, Finch D, Kreith F, Mahajan RL, Norris DA. Fast response temperature measurement and highly reproducible heating methods for 96-well plates. BioTechniques. 2004;36(6):968–76.
30. Debes A, Willers R, Göbel U, Wessalowski R. Role of heat treatment in childhood cancers: Distinct resistance profiles of solid tumor cell lines towards combined thermochemotherapy. Pediatr Blood Cancer. 2005;45(5):663–9.
31. Herea DD, Danceanu C, Radu E, Labusca L, Lupu N, Chiriac H. Comparative effects of magnetic and water-based hyperthermia treatments on human osteosarcoma cells. Int J Nanomedicine. 2018;13:5743–51.
32. Massey AJ. A high content, high throughput cellular thermal stability assay for measuring drug-target engagement in living cells. PLoS One. 2018;13(4):e0195050.
33. Amini SM, Kharrazi S, Jaafari MR. Radio frequency hyperthermia of cancerous cells with gold nanoclusters: An in vitro investigation. Gold Bull. 2017;50(1):43–50.
34. Ware MJ, Krzykawska-Serda M, Chak-Shing Ho J, Newton J, Suki S, Law J, Nguyen L, Keshishian V, Serda M, Taylor K, Curley SA, Corr SJ. Optimizing non-invasive radiofrequency hyperthermia treatment for improving drug delivery in 4T1 mouse breast cancer model. Sci Rep. 2017;7(1):43961.
35. Yang D, Converse MC, Mahvi DM, Webster JG. Measurement and analysis of tissue temperature during microwave liver ablation. IEEE Trans Biomed Eng. 2007;54(1):150–5.
36. Philips P, Scoggins CR, Rostas JK, McMasters KM, Martin RC. Safety and advantages of combined resection and microwave ablation in patients with bilobar hepatic malignancies. Int J Hypothermia. 2017;33(1):43–50.
37. Choi SH, Kim JW, Kim JH, Kim KW. Efficacy and safety of microwave ablation for malignant renal tumors: An updated systematic review and meta-analysis of the literature since 2012. Korean J Radiol. 2018;19(5):938–49.
38. Yu Z, Geng J, Zhang M, Zhou Y, Fan Q, Chen J. Treatment of osteosarcoma with microwave thermal ablation to induce immunogenic cell death. Oncotarget. 2014;5(15):6526–39.
39. Manderson CA, McLiesh H, Curvello R, Tabor RF, Manolios J, Garnier G. Photothermal incubation of red blood cells by laser for rapid pre-transfusion blood group typing. Sci Rep. 2019;9(1):11221.
40. Miura Y, Pruessner J, Mertineit CL, Kern K, Muenter M, Moltmann M, Danicke V, Brinkmann R. Continuous-wave thulium laser for heating cultured cells to investigate cellular thermal effects. J Vis Exp. 2017;(124):54326.
41. Mu C, Wu X, Zhou X, Wolfram J, Shen J, Zhang D, Mai J, Xia X, Holder AM, Ferrari M, Liu X, Shen H. Chemotherapy sensitizes therapy-resistant cells to mild hyperthermia by suppressing heat shock protein 27 expression in triple-negative breast cancer. Clin Cancer Res. 2018;24(19):4900–12.
42. Shirata C, Kaneko J, Inagaki Y, Kokudo T, Sato M, Kiritani S, Akamatasu N, Arita J, Sakamoto Y, Hasegawa K, Kokudo N. Near-infrared photothermal/photodynamic therapy with indocyanine green induces apoptosis of hepatocellular carcinoma cells through oxidative stress. Sci Rep. 2017;7(1):13958.
43. Bani MS, Hatamie S, Haghpanahi M, Bahreinizad H, Alavijeh MHS, Eivazzadeh-Keihan R, Wei ZH. Casein-coated iron oxide nanoparticles for in vitro hyperthermia for cancer therapy. SPIN. 2019;09(02):1940003.
44. Ito A, Tanaka K, Kondo K, Shinkai M, Honda H, Matsumoto K, Saida T, Kobayashi T. Tumor regression by combined immunotherapy and hyperthermia using magnetic nanoparticles in an experimental subcutaneous murine melanoma. Cancer Sci. 2003;94(3):308–13.
45. Brüningk SC, Rivens I, Mouratidis P, ter Haar G. Focused ultrasound-mediated hyperthermia in vitro: An experimental arrangement for treating cells under tissue-mimicking conditions. Ultrasound Med Biol. 2019;45(12):3290–7.
46. Vanherberghen B, Manneberg O, Christakou A, Frisk T, Ohlin M, M. Hertz H, Wiklund M, Onfelt B. Ultrasound-controlled cell aggregation in a multi-well chip. Lab Chip. 2010;10(20):2727–32.
47. Mylonopoulou E, Bazán-Peregrino M, Arvanitis CD, Coussios CC. A non-exothermic cell-embedding tissue-mimicking material for studies of ultrasound-induced hyperthermia and drug release. Int J Hypothermia. 2013;29(2):133–44.
48. Bridle H, Millingen M, Jesorka A. On-chip fabrication to add temperature control to a microfluidic solution exchange system. Lab Chip. 2008;8(3):480–3.
49. Picard C, Hearnden V, Massignani M, Achouri S, Battaglia G, MacNeil S, Donald A. A micro-incubator for cell and tissue imaging. Biotechniques. 2010;48(2):135–8.
50. Mouratidis PXE, Rivens I, ter Haar G. A study of thermal dose-induced autophagy, apoptosis and necroptosis in colon cancer cells. Int J Hypothermia. 2015;31(5):476–88.

51. Nytko KJ, Thumser-Henner P, Weyland MS, Scheidegger S, Bley CR. Cell line-specific efficacy of thermoradiotherapy in human and canine cancer cells in vitro. PLoS One. 2019;14(5):e0216744.
52. Mantso T, Vasileiadis S, Anestopoulos I, Voulgaridou GP, Lampri E, Botaitis S, Kontomanolis EN, Simopoulos C, Franco R, Chlichlia K, Pappa A, Panayiotidis MI. Hyperthermia induces therapeutic effectiveness and potentiates adjuvant therapy with non-targeted and targeted drugs in an in vitro model of human malignant melanoma. Sci Rep. 2018;8(1):10724.
53. Lee H, Park HJ, Park CS, Oh ET, Choi BH, Williams B, Lee CK, Song CW. Response of breast cancer cells and cancer stem cells to metformin and hyperthermia alone or combined. PLoS One. 2014;9(2):e87979.
54. Jiang W, Bian L, Wang N, He Y. Proteomic analysis of protein expression profiles during hyperthermia-induced apoptosis in Tca8113 cells. Oncol Lett. 2013;6(1):135–43.
55. Beck BD, Dynlacht JR. Heat-induced aggregation of XRCC5 (Ku80) in nontolerant and thermotolerant cells. Radiat Res. 2001;156(6):767–74.
56. Yang KL, Huang CC, Chi MS, Chiang HC, Wang YS, Hsia CC, Andocs G, Wang HE, Chi KH. In vitro comparison of conventional hyperthermia and modulated electro-hyperthermia. Oncotarget. 2016;7(51):84082–92.
57. Rylander MN, Diller KR, Wang S, Aggarwal SJ. Correlation of HSP70 expression and cell viability following thermal stimulation of bovine aortic endothelial cells. J Biomech Eng. 2005;127(5):751–7.
58. Reddy G, Dreher MR, Rossmann C, Wood BJ, Haemmerich D. Cytotoxicity of hepatocellular carcinoma cells to hyperthermic and ablative temperature exposures: In vitro studies and mathematical modelling. Int J Hypothermia. 2013;29(4):318–23.
59. Kiourti A, Sun M, He X, Volakis JL. Microwave cavity with controllable temperature for in vitro hyperthermia investigations. J Electromagn Eng Sci. 2014;14(3): 267–72.
60. Zhao YY, Wu Q, Wu ZB, Zhang JJ, Zhu LC, Yang Y, Ma SL, Zhang SR. Microwave hyperthermia promotes caspase-3-dependent apoptosis and induces G2/M checkpoint arrest via the ATM pathway in non-small cell lung cancer cells. Int J Oncol. 2018;53(2):539–50.
61. Manop P, Keangin P, Nasongkla N, Eawsakul K. In vitro experiments of microwave ablation in liver cancer cells (effects of microwave power and heating time), 2020 IEEE 7th International Conference on Industrial Engineering and Applications (ICIEA); 2020. p. 805–13.
62. Asano M, Sakaguchi M, Tanaka S, Kashimura K, Mitani T, Kawase M, Matsumura H, Yamaguchi T, Fujita Y, Tabuse K. Effects of normothermic conditioned microwave irradiation on cultured cells using an irradiation system with semiconductor oscillator and thermo-regulatory applicator. Sci Rep. 2017;7(1):41244.
63. Chen L, Wang M, Lin Z, Yao M, Wang W, Cheng S, Li B, Zhang Y, Yin Q. Mild microwave ablation combined with HSP90 and TGF-β1 inhibitors enhances the therapeutic effect on osteosarcoma. Mol Med Rep. 2020;22(2):906–14.
64. Schwartz JA, Shetty AM, Price RE, Stafford RJ, Wang JC, Uthamanthil RK, Pham K, McNichols RJ, Coleman CL, Payne JD. Feasibility study of particle-assisted laser ablation of brain tumors in orthotopic canine model. Cancer Res. 2009;69(4):1659–67.
65. Schena E, Saccomandi P, Fong Y. Laser ablation for cancer: Past, present and future. J Funct Biomater. 2017;8(2):19.
66. Inagaki K, Shuo T, Katakura K, Ebihara N, Murakami A, Ohkoshi K. Sublethal photothermal stimulation with a micropulse laser induces heat shock protein expression in ARPE-19 cells. J Ophthalmol. 2015;2015:729792.
67. Tang F, Zhang Y, Zhang J, Guo J, Liu R. Assessment of the efficacy of laser hyperthermia and nanoparticle-enhanced therapies by heat shock protein analysis. AIP Advances. 2014;4(3):031334.
68. Lins EC, Oliveira CF, Guimarães OCC, Costa CA de S, Kurachi C, Bagnato VS. A novel 785-nm laser diode-based system for standardization of cell culture irradiation. Photomed Laser Surg. 2013;31(10):466–73.
69. Liljemalm R, Nyberg T, Holst H von. Heating during infrared neural stimulation. Lasers Surg Med. 2013;45(7):469–81.
70. Tang Y, McGoron AJ. Increasing the rate of heating: A potential therapeutic approach for achieving synergistic tumour killing in combined hyperthermia and chemotherapy. Int J Hypothermia. 2013;29(2):145–55.
71. Murat FJ, Poissonnier L, Pasticier G, Gelet A. High-intensity focused ultrasound (HIFU) for prostate cancer. Cancer Control. 2007;14(3):244–9.
72. So MJ, Fennessy FM, Zou KH, McDannold N, Hynynen K, Jolesz FA, Stewart EA, Rybicki F, Tempany CM. Does the phase of menstrual cycle affect MR-guided focused ultrasound surgery of uterine leiomyomas? Eur J Radiol. 2006;59(2):203–7.
73. Kennedy JE. High-intensity focused ultrasound in the treatment of solid tumours. Nat Rev Cancer. 2005;5(4):321–7.
74. Sapareto SA, Hopwood LE, Dewey WC, Raju MR, Gray JW. Effects of hyperthermia on survival and progression of Chinese hamster ovary cells. Cancer Res. 1978;38(2):393–400.
75. Horsman MR, Overgaard J. Hyperthermia: A potent enhancer of radiotherapy. Clin Oncol. 2007;19(6):418–26.
76. Zhang X, Bobeica M, Unger M, Bednarz A, Gerold B, Patties I, Melzer A, Landgraf L. Focused ultrasound radiosensitizes human cancer cells by enhancement of DNA damage. Strahlenther Onkol. 2021;197(8):730–43.
77. Mäki AJ, Verho J, Kreutzer J, Ryynänen T, Rajan D, Pekkanen-Mattila M, Ahola A, Hyttinen J, Setala KA, Lekkala J, Kallio P. A portable microscale cell culture system with indirect temperature control. SLAS Technol. 2018;23(6):566–79.
78. Regalia G, Biffi E, Achilli S, Ferrigno G, Menegon A,

Pedrocchi A. Development of a bench-top device for parallel climate-controlled recordings of neuronal cultures activity with microelectrode arrays. Biotechnol Bioeng. 2016;113(2):403–13.
79. Lin JL, Wu MH, Kuo CY, Lee KD, Shen YL. Application of indium tin oxide (ITO)-based microheater chip with uniform thermal distribution for perfusion cell culture outside a cell incubator. Biomed Microdevices. 2010;12(3):389–98.
80. Vukasinovic J, Cullen DK, LaPlaca MC, Glezer A. A microperfused incubator for tissue mimetic 3D cultures. Biomed Microdevices. 2009;11(6):1155–65.
81. Petronis S, Stangegaard M, Christensen CBV, Dufva M. Transparent polymeric cell culture chip with integrated temperature control and uniform media perfusion. Biotechniques. 2006;40(3):368–76.
82. Lin L, Wang SS, Wu MH, Oh-Yang CC. Development of an integrated microfluidic perfusion cell culture system for real-time microscopic observation of biological cells. Sensors. 2011;11(9):8395–411.
83. Nieto D, McGlynn P, de la Fuente M, Lopez-Lopez R, O'Connor GM. Laser microfabrication of a microheater chip for cell culture outside a cell incubator. Colloids Surf B Biointerfaces. 2017;154:263–9.
84. Cheng JY, Yen MH, Kuo CT, Young TH. A transparent cell-culture microchamber with a variably controlled concentration gradient generator and flow field rectifier. Biomicrofluidics. 2008;2(2):024105.
85. Whitesides GM. The origins and the future of microfluidics. Nature. 2006;442(7101):368–73.
86. Halldorsson S, Lucumi E, Gómez-Sjöberg R, Fleming RMT. Advantages and challenges of microfluidic cell culture in polydimethylsiloxane devices. Biosens Bioelectron. 2015;63:218–31.
87. Mehling M, Tay S. Microfluidic cell culture. Curr Opin Biotechnol. 2014;25:95–102.
88. Lagally ET, Emrich CA, Mathies RA. Fully integrated PCR-capillary electrophoresis microsystem for DNA analysis. Lab Chip. 2001;1(2):102–7.
89. Khandurina J, McKnight TE, Jacobson SC, Waters LC, Foote RS, Ramsey JM. Integrated System for rapid PCR-based DNA analysis in microfluidic devices. Anal Chem. 2000;72(13):2995–3000.
90. Mello AJ de, Habgood M, Lancaster NL, Welton T, Wootton RCR. Precise temperature control in microfluidic devices using Joule heating of ionic liquids. Lab Chip. 2004;4(5):417–9.
91. Burke C, Dreher MR, Negussie AH, Mikhail AS, Yarmolenko P, Patel A, Skilskyj B, Wood BJ, Haemmerich D. Drug release kinetics of temperature sensitive liposomes measured at high-temporal resolution with a millifluidic device. Int J Hypothermia. 2018;34(6): 786–94.
92. Cantoni F, Werr G, Barbe L, Porras AM, Tenje M. A microfluidic chip carrier including temperature control and perfusion system for long-term cell imaging. HardwareX. 2021 Oct 1;10:e00245.
93. Ross D, Gaitan M, Locascio LE. Temperature measurement in microfluidic systems using a temperature-dependent fluorescent dye. Anal Chem. 2001;73(17):4117–23.
94. Hahn GM. Hyperthermia for the engineer: A short biological primer. IEEE Trans Biomed Eng. 1984;BME-31(1):3–8.
95. Henle KJ, Leeper DB. Interaction of hyperthermia and radiation in CHO cells: Recovery kinetics. Radiat Res. 1976;66(3):505–18.
96. Mouratidis PXE, Rivens I, Civale J, Symonds-Tayler R, ter Haar G. Relationship between thermal dose and cell death for "rapid" ablative and "slow" hyperthermic heating. Int J Hypothermia. 2019;36(1):228–42.
97. Miura Y, Seifert E, Rehra J, Kern K, Theisen-Kunde D, Denton M, Brinkmann R. Real-time optoacoustic temperature determination on cell cultures during heat exposure: A feasibility study. Int J Hyperthermia. 2019;36(1):466–72.
98. Haemmerich D, Santos I dos, Schutt DJ, Webster JG, Mahvi DM. In vitro measurements of temperature-dependent specific heat of liver tissue. Med Eng Phys. 2006;28(2):194–7.
99. Coombe AR, Ho CTG, Darendeliler MA, Hunter N, Philips JR, Chapple CC, Yum LW. The effects of low level laser irradiation on osteoblastic cells. Clin Orthod Res. 2001;4(1):3–14.
100. Fisher JW, Sarkar S, Buchanan CF, Szot CS, Whitney J, Hatcher HC, Torti SV, Rylander CG, Rylander MN. Photothermal response of human and murine cancer cells to multiwalled carbon nanotubes after laser irradiation. Cancer Res. 2010;70(23):9855–64.
101. Ertel SI, Ratner BD, Kaul A, Schway MB, Horbett TA. In vitro study of the intrinsic toxicity of synthetic surfaces to cells. J Biomed Mater Res. 1994;28(6):667–75.
102. Song AS, Najjar AM, Diller KR. Thermally induced apoptosis, necrosis, and heat shock protein expression in 3D culture. J Biomech Eng. 2014;136(7):10.1115/1.4027272.
103. Ji Z, Ma Y, Zhao H, Li W, Li X, Yun Z, Zhao G, Ma B, Fan Q. The effect of temperature-control microwave on HELA and MG-63 cells. J Cancer Res Ther. 2018;14(Suppl):S152–8.
104. Guo C, Yin S, Yu H, Liu S, Dong Q, Goto T, Zhang Z, Li Y, Sato T. Photothermal ablation cancer therapy using homogeneous CsxWO3 nanorods with broad near-infra-red absorption. Nanoscale. 2013;5(14):6469–78.
105. Dunn AW, Ehsan SM, Mast D, Pauletti GM, Xu H, Zhang J, Ewing RC, Shi D. Photothermal effects and toxicity of Fe3O4 nanoparticles via near infrared laser irradiation for cancer therapy. Mater Sci Eng C Mater Biol Appl. 2015;46:97–102.
106. Lai CY, Kruse DE, Caskey CF, Stephens DN, Sutcliffe PL, Ferrara KW. Noninvasive thermometry assisted by a dual-function ultrasound transducer for mild hyperthermia. IEEE Trans Ultrason Ferroelectr Freq Control. 2010;57(12):2671–84.

107. Heidemann SR, Lamoureux P, Ngo K, Reynolds M, Buxbaum RE. Open-dish incubator for live cell imaging with an inverted microscope. BioTechniques. 2003;35(4):708–16.
108. Byers KM, Lin LK, Moehling TJ, Stanciu L, Linnes JC. Versatile printed microheaters to enable low-power thermal control in paper diagnostics. Analyst. 2019;145(1):184–96.
109. Wu J, Cao W, Wen W, Chang DC, Sheng P. Polydimethylsiloxane microfluidic chip with integrated microheater and thermal sensor. Biomicrofluidics. 2009;3(1):012005.